

# Modelling urban stormwater drainage overflows for assessing flood hazards Detection of flooding by overflows of the drainage network: **Application to the urban area of Dakar (Senegal)**

Laurent Pascal Malang Diémé<sup>1,2</sup>, Christophe Bouvier<sup>2</sup>, Ansoumana Bodian<sup>1</sup> and Alpha Sidibé<sup>3</sup>

5 <sup>1</sup> Laboratoire Leïdi “Dynamique des Territoires et Développement”, Université Gaston Berger (UGB), Saint Louis, Sénégal

<sup>2</sup> IRD, UMR 5151, HSM, Univ. Montpellier, CNRS, IRD, Montpellier, France

<sup>3</sup>DPGI “Direction de la Prévention et de la Gestion des Inondations au Sénégal”, MEA, Sénégal

*Correspondence to:* Laurent P. M. Diémé (dieme.laurent-pascal-malang@ugb.edu.sn)

## **Abstract.**

10 With the recurrence of flooding in African cities, there is growing interest in ~~the development of~~ developing sufficiently informative tools to help characterize and predict overflow risks. One of the challenges is to develop methods that strike a compromise between the accuracy of simulations, the availability of basic data, and the shortening of calculation times to be compatible with real-time applications. The present study, carried out on the urban outskirts of Dakar, aims to propose a method capable of ~~modeling-modelling~~ flows at fine resolution ( $25\text{m}^2$ ), over the entire area, and providing a rapid diagnosis

15 of how the drainage network is operating for rainfall intensities of different return periods, while taking urban conditions into account. Three methodological steps are combined to achieve this objective: (i) determination of drainage directions, including modifications induced by buildings, artificial drainage, and storage basins, (ii) application of a hydrological model for calculating flows at the outlets of elementary catchment, (iii) ~~the~~ implementation of a hydraulic model for propagating these flows through the drainage network and a storage model for retention basins. The modelling chain was built within the

20 ATHYS platform. The network overflow points are detected if ~~calculated as~~ the difference between the calculated flows exceed and the network's capacity to evacuate them. Examples are given by carrying out simulations using 10 and 100-years design rainfall. Simulation results show that the stormwater drainage network is capable of evacuating runoff volumes generated by rainfall with a low return period (10 years), but seems to overflow for rainfall with a rare frequency (100 years), with overflow rates sometimes exceeding  $18\text{ m}^3/\text{s}$ . The model, ~~built on the ATHYS modelling platform,~~ also provides

25 boundary conditions for applying more complex hydraulic models to determine the local impact of drainage network overflows on limited areas. However, the goodness of the method still needs to be validated in further research by comparing with accurate data from observed flood events.

## 1 Introduction

African cities are frequently subject to flooding (Yengoh et al., 2017; Tazen et al., 2018; Sy et al., 2020; Barau and Wada, 2021), which results in significant socio-economic, health, and environmental damage (Miller et al., 2022a; Sakijege and Dakyaga, 2023). The current trend ~~towards-toward~~ more intense rainfall (Taylor et al., 2017; Bichet and Diedhiou, 2018; Nkrumah et al., 2019; Klutse et al., 2021), attributed to climate change (Panthou et al., 2018; Chagnaud et al., 2022) and the very rapid dynamics of ~~urbanisation-urbanization~~ (Sène, 2018; Williams et al., 2019; Yuan et al., 2023), are expected to increase the ~~occurrence recurrence~~ of urban flooding (Gaisie and Cobbinah, 2023). This is a major source of concern for political decision-makers and city dwellers (Moulds et al., 2021) in these African conurbations, where the gap between adaptation needs and existing tools is wide (Nkwunonwo et al., 2020; Miller, et al., 2022b).

In response to growing adaptation needs (Kreibich et al., 2017; Mashi et al., 2020), interest is being shown in flood characterization (Coulibaly et al., 2020) and forecasting (Chen et al., 2015). ~~In this respect, the~~The scientific literature reports on several methods implemented, in urban environments, to provide flood assessment and mapping (Henonin et al., 2013; Agonafir et al., 2023). The simplest methods, without introducing simulations of runoff formation, rely on the topographical characteristics of the territory to give a first local estimate of flood risk by ~~the~~ accumulation of water at low points (Pons et al., 2010; Dehotin et al., 2015; Zheng et al., 2018). ~~As for the~~1D hydrological and hydraulic ~~modelingmodelling~~ approach, well established in the literature (Zhu et al., 2016; Rabori and Ghazavi, 2018; Sidek et al., 2021; Chahinian et al., 2023), ~~it is are also~~ applied to simulate stormwater drainage network performance (Meng et al., 2019; Pla et al., 2019). ~~ModelingModelling~~ platforms such as SWMM (Rossman, 2015; Rabori and Ghazavi, 2018) or InfoWorks ICM are 1D simulation tools applied in urban environments (Rubinato et al., 2013; Sidek et al., 2021). However, this type of ~~modelingmodelling~~, which is essentially one-dimensional, does not provide spatial propagation of overflow water (Mark et al., 2004). ~~However, this type of modeling, which is essentially one dimensional, does not provide the spatial propagation of overflow water (Mark et al., 2004).~~ This aspect is taken into account by 2D models such as Mike Urban (DHI, 2021). The accuracy of the simulations they can provide on the spatial propagation of surface flows is limited by ~~both~~ their numerical complexity, ~~to which is added the fine quality of the and the required~~ data (fine topographic mesh, physical and urban characteristics) ~~required~~ for their parameterization (Costabile et al., 2020; Zanchetta and Coulibaly, 2020). These 2D or coupled 1D-2D models (Martínez et al., 2018; Bulti and Abebe, 2020; Li et al., 2022) require substantial computing resources, long calculation times and are difficult to apply over large areas or for real-time flood forecasting studies (Rosenzweig et al., 2021). Today, ~~we are also witnessing~~ the emergence of increasingly used AI (artificial intelligence) / ML (machine learning) ~~machine learning~~ techniques (Mosavi et al., 2018; Darabi et al., 2019), ~~which have offers~~ the ~~potential possibility of to provide-providing~~ flood mapping through model training (Mosavi et al., 2018; Darabi et al., 2019; Parvin et al., 2022; Taromideh et al., 2022). Their application can be challenging as they generally require a large amount of data (meteorological, hydrological, topographical) to be integrated for training, ~~in order toto~~ improve accuracy and achieve good model performance (Bentivoglio et al., 2022).

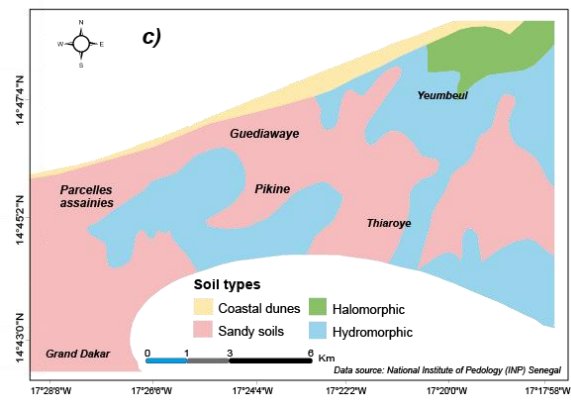
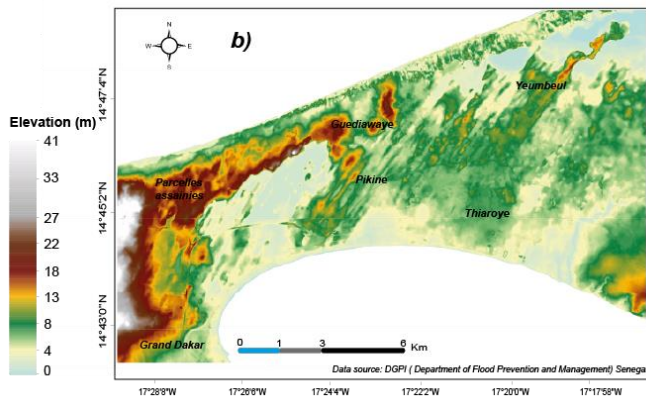
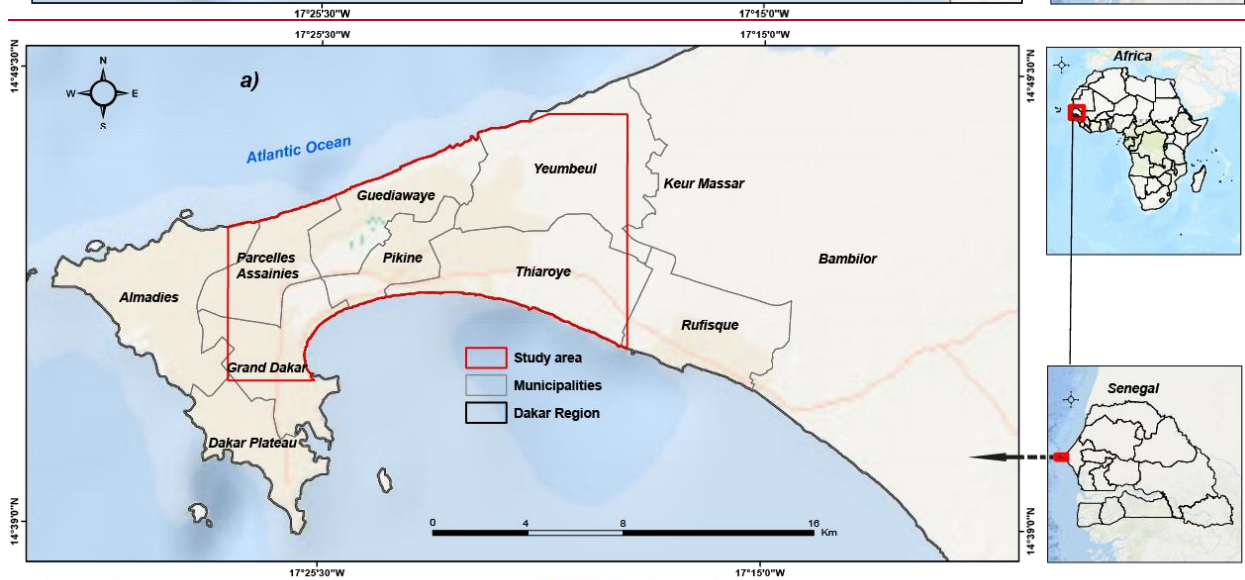
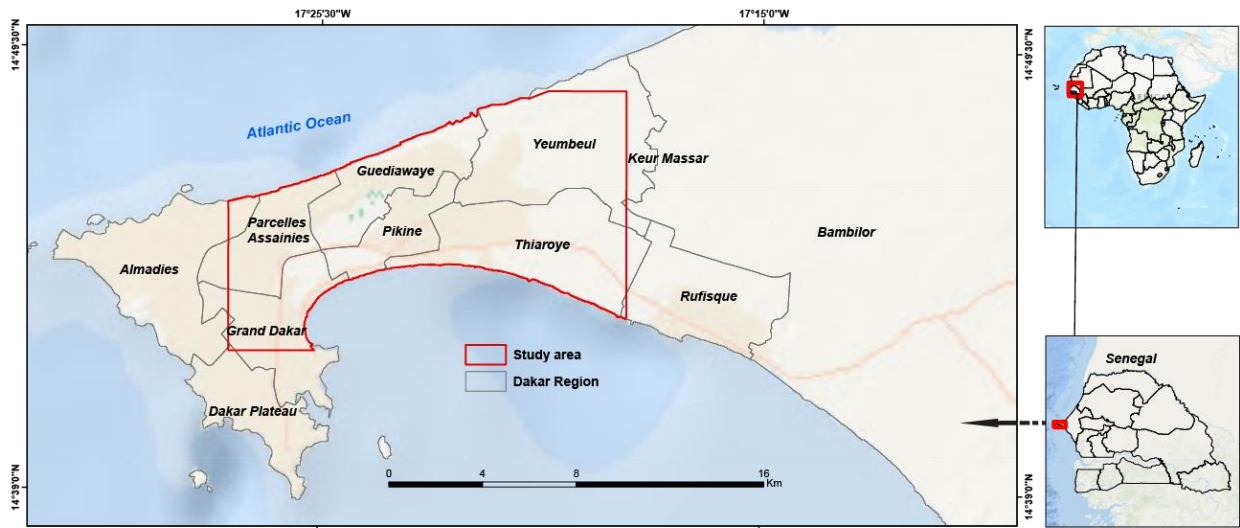
In urban environments, one of the main factors influencing the choice of an appropriate modelling approach is data availability ~~and the flooding context~~ (Henonin et al., 2013). ~~For In~~ the African context, where the availability of detailed data is ~~scarcerare~~, the challenge is to implement alternative solutions by finding a compromise between the availability of basic data, the reduction of calculation times, and the accuracy of flood simulations (Chahinian et al., 2023). ~~The aim of this study is~~ This study aims to propose fine-resolution ( $25\text{m}^2$ ) modelling of flows and overflows from drainage and storage ~~network network over a large area (~400 km<sup>2</sup>) in on the scale of the~~ Dakar's urban periphery, with short calculation times (5mn) compatible with real-time applications. The proposed methodological approach follows three main stages: (i) ~~the~~ reconstruction of urban drainage directions, taking into account the modifications caused by the various urban developments (buildings, artificial channels, and retention basins), using algorithms developed for this purpose, (ii) calculation of flows ~~from small elementary catchments in project mode~~, using a parsimonious hydrological model (SCS-LR) adapted to the local context, which in particular integrates the density of ~~urbanisationurbanization on the scale of small basins~~, combined with (iii) a 1D hydraulic model for propagating these flows through the drainage network and a storage model for retention basins. The overflow points ~~in the drainage network~~ are identified by the difference between the maximum flows produced and the network's capacity to evacuate them. This work is structured in four parts. First, the study area ~~and the used datasets are is~~ described, then ~~the data and~~ the detailed structure of the method ~~are is~~ presented, followed by the model ~~parameterisationparameterization~~ strategy and finally, ~~two examples of simulation using a 10 and 100-year design storm are given and discussed the results and a discussion~~ highlighting possible improvements, before concluding.

## 2 Study area ~~and datasets~~

### 2.1 Study area

~~The study area is located in the peri-urban of Dakar (Fig. 1a), capital of Senegal. Dakar (Fig. 1), the capital of Senegal concentrates almost ¼ of the country's total population on just 0.3% of the national territory (ANSD, 2013). Its urbanization This part of the city is characterized by a relatively flat relief (Fig. 1b), consisting of a series of small coastal dunes interspersed with wet depressions - called Niayes - that have dried up during the drought of the 1970s in the Sahelian zone (Nicholson et al., 2000). In the study area, the natural drainage network is temporary and has largely fossilized (Bassel, 1996). A major part of the soils is sandy in the dunes. Hydromorphic soils dominate the area around the depressions (Fig. 1c) given the proximity of the water table in some places (Cissé Faye et al., 2004). Dakar experiences extreme variations in monthly rainfall throughout the year. The rainy season last for 4 months, from June to September. August and September receive the highest amount of rain. Over the period 1988 to 2018, annual rainfall varies between 161 mm and 660 mm, with an average of 402 mm which is a characteristic of a tropical semi-arid zone. The urbanization of this peri-urban area took place rapidly since, in the space of a few decades, It was largely fuelled by the rural exodus (Lericollais and Roquet, 1999) following the drought of the 1970s (Nicholson et al., 2000). This resulted in rapid population growth and a dense occupation of space helped by, with the establishment of the network of roads to facilitate~~

urban mobility (Ndiaye, 2015), ~~the land reserves of the distant eastern periphery have been invaded and densely urbanised (Lessault and Imbert, 2013). This Moreover, settlement~~ is sometimes achieved through (i) the infilling of former drained  
95 wetland depressions (Sène et al., 2018), (ii) self-occupation practices, without ~~taking into account considering~~ –the  
topography of the land, the hydrology -or the installation of rainwater drainage structures (Ndiaye, 2015).



100 **Figure 1: a) Location of the study area; b) Digital Terrain Model (DTM); c) soil type distribution**

From the 2000s onwards, there was a return of rainfall (Sene and Ozer, 2002; Bodian, 2014; Nouaceur, 2020) after a period of drought, causing that caused a series of floods in Dakar (Bottazzi et al., 2018; Hungerford et al., 2019). The most significant episodes are generally noted during the critical rainy periods in August and September: august 2005, September 2009, August 2012; August 2015, September 2020, August 2021, and recently August 2022. On 26 August 2012, for  
105 example, 161 mm of rain fell in less than 2 hours, including 144 mm in 51 minutes (Descroix et al., 2013) which had a serious impact on the population, resulting in 26 deaths (Sané et al., 2016) and causing pandemics such as cholera and malaria (Magny et al., 2012; Sambe-Ba et al., 2013). One of the government's responses was to set up a vast programmeprogram, including the Stormwater Management and Climate Change Adaptation project (PROGEP), which since 2012 has aimed to build drainage networks linked to storage basins to minimise-minimize the risks (Diop, 2019).

110

One of the current challenges for urban management, in a-the context of increasing intense rainfall, dense urbanisation urbanization and infrastructure development, is to develop effective and robust tools to support flood assessment and decision-making.

## 2.2 Datasets

115 2.2.1 Geographic datasets

The geographical datasets required to reconstruct the modified urban drainage directions (Diémé et al., 2022) are compiled in an urban database for Dakar by the Senegal Flood Prevention and Management Department (DPGI) and the Geography and Cartography Department (DTGC). These include the DTM, the location of buildings, rainwater channels, and retention basins. The 10m resolution DTM, that we resampled to 5m, is specifically produced for the city of Dakar by the National  
120 Institute for Geographic and Forestry Information (IGN) of France, using the photogrammetric restitution technique. The buildings layer was created by manually digitizing high-resolution (50 cm) satellite images. The location and characteristics of the channels (width, depth) and retention basins (storage volume, leakage rate) are provided in the various technical reports supplied by the PROGEP project. The majority of channels are surface drains and are rectangular. All the known characteristics of the channels and the dimensions of the retention basins have been referenced for use in calibrating the  
125 hydraulic models.

## 2.2.2 IDF curves

The available IDF curves used in this study were derived from the GEV law parameters calculated by Sane et al. (2018), for each region of Senegal using long-term historical rainfall data from 23 tipping bucket rain gauges (Bodian et al., 2016). These historical data range from 1955 to 2005. To obtain a reliable estimate of the GEV distribution parameters  $\mu$ ,  $\sigma$  and  $\varepsilon$   
130 for each rainfall station, all the rainfall of different durations  $d$  were merged, considering that the rainfalls of any duration  $d$

are identically distributed with a scaling factor  $\eta$ . This approach made it possible to estimate the GEV parameters (Eq. 1, 2, and 3) of the distribution of the rainfalls of any duration  $d$  as:

$$\mu(d) = \mu \cdot d^\eta \quad (1)$$

$$\sigma(d) = \sigma \cdot d^\eta \quad (2)$$

135  $\varepsilon(d) = \varepsilon \quad (3)$

with  $\mu = 28.9$  mm,  $\sigma = 12.5$  mm,  $\varepsilon = 0.08$ , with  $\eta$  set to  $\eta = -0.86$ .

Application of Eq. 4 allow to determine a value  $x$  knowing his return period  $T$ .

$$x = \mu + \frac{\sigma}{\varepsilon} \left( -1 + \left( -\ln \left( 1 - \frac{1}{T} \right) \right)^{-\varepsilon} \right) \quad (4)$$

For different return period (years), the rainfalls of duration  $d$  between 1 and 24 hours were then given by Table 1

140 **Table: Summary of Dakar IDF curves calculated from GEV parameters defined by Sane et al. (2018).**

Duration (hrs)	Return period (yrs)					
	2yr $i_T$ mm/hr	5yr $i_T$ mm/hr	10yr $i_T$ mm/hr	20yr $i_T$ mm/hr	50yr $i_T$ mm/hr	100yr $i_T$ mm/hr
1	34.4	49.7	60.6	71.7	87	99.3
2	18.9	27.2	33.1	39.1	47.5	54.2
4	10.3	14.8	18.1	21.4	25.9	29.5
6	7.2	10.4	12.7	15	18.2	20.7
9	5.1	7.3	8.9	10.5	12.7	14.5
12	4	5.7	6.9	8.1	9.9	11.2
24	2.1	3.1	3.8	4.5	5.5	6.3

### 3 Data and method ~~Method~~ presentation

The detailed methodological approach ~~followed~~ is structured in seven successive ~~stages~~ steps (Fig. 2). The first ~~step~~ is (i) the construction of the natural drainage topology modified by urban objects, (ii) on which is based the division of the urban area into small elementary catchment areas and the extraction of the associated hydrographic network. Then (iii) a ~~rainfall-runoff hydrological production and routing~~ model is applied to calculate the hydrographs at the outlets of the elementary ~~catchment~~basins. These hydrographs are (iv) propagated in the storm~~water~~ drainage network by a 1D hydraulic model and (v) their ~~conservation~~ storage in the retention basins is managed by a ~~storage~~ linear reservoir model. Finally, (vi) ~~project rainfalls~~ design storms are ~~constructed~~ derived from local Intensity-Duration-Frequency (IDF) curves and ~~used as input data~~

145

150 ~~to injected in~~ the model, which is then (vii) implemented to detect, over the entire study area, the overflow points of the drainage and storage network according to different levels of severity and urban density.

The modelling chain was built in the ATHYS platform, developed by Hydrosiences Montpellier. ATHYS enables a range of hydrological and hydraulic GIS-based models (MERCEDES unit), as well as geographical (VICAIR unit) and hydrometeorological (VISHYR unit) data processors. ATHYS is a free software, available from [www.athys-soft.org](http://www.athys-soft.org). The

155 entire processing chain and the associated data are presented in detail in the following sections.

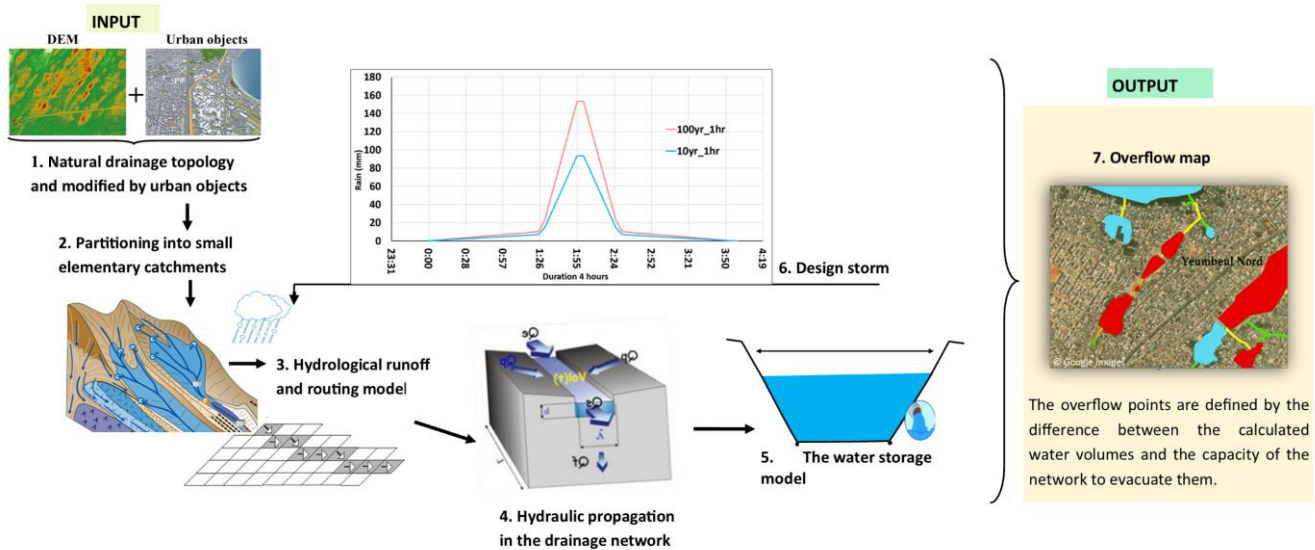


**Figure 2: Flow chart of the methodology**

### 3.1 Construction of the drainage ~~topologietopology~~

160 The construction of the drainage topology, which aims aimed at reconstructing the modified drainage directions of run-off water, is a prerequisite to the implementation of the overflow point detection model. The natural path flows can be easily derived from the 5m-DTM, but in urban areas, the natural flows must be modified by artificial objects such as buildings, channels, and retention basins. This topology construction methodology was previously applied to the study area (Diémé et al., 2022), and can be summarized in 3 steps :

- 165
- modification of the elevation of the urban blocks (e.g. 25m) and extraction of the flow paths from the modified 5m-DTM (Jenson and Domingue, 1988),
  - modification of flow paths according to the artificial channel network: The VICAIR algorithm uses a raster map of the channels, detects all the nodes of the channel network, and modifies the flow paths of each channel from the upstream node to the downstream node. The upstream and downstream nodes are recognized by their elevation in the DTM



170 ~~b)c) modification of the flow paths in the retention basins: The VICAIR algorithm uses a raster map of the basins, detects the outlet of the basin as being the channel that drains out the basin, and modifies all the flow paths of the basin towards the outlet.~~

175 ~~e) . using spatial data from the Dakar urban database compiled by the Senegal flood prevention and management department (DPGI) and the Geographic Works and Cartography Department (DTGC). It is based on a fine resolution DTM (10m, resampled to 5m), From which natural drainage directions are extracted (Jenson and Domingue, 1988). These drainage directions are then forced to produce an associated drainage model that incorporates (i) the presence of buildings, (ii) collectors and (iii) retention basins. These operations were carried out using a combination of GIS tools and the Vicair module of the ATHYS modelling platform (<http://www.athys-soft.org/>), where specific algorithms were developed for this purpose (see Diémé et al. (2022) for more details).(Laganier et al., 2014; Aqnouy et al., 2023)~~

### 3.2 Partitioning the study area into elementary ~~catchments basins~~ and networks

185 The modified drainage model was first used to reconstitute elementary catchments and channel networks. Building elementary catchments and channel networks is necessary to save time on computation as well as connect both hydrological and hydraulic models. The elementary catchments were defined as catchments with the same ~~urbanised-urbanized~~ area. A threshold of 10 hectares (ha) was adopted for this ~~urbanised-urbanized~~ area. Thus catchments can be small (10 ha if totally urbanized) or larger (if the catchment is mostly natural). This allows to reduce the number of elementary catchments in the natural areas, without loss of accuracy regarding the channel network behaviour in the urban areas.

190 The criteria for delineating delimiting these ~~small catchments basins~~ are taken from Jenson and Domingue (1988). They consist ~~in-of~~ marking the mesh as the outlet of a basin if:

- its urbanized drained area is greater than N (here 10ha)
- the difference in urbanized drained area between this mesh and the downstream mesh is greater than N.

195 ~~In this way~~ Thus, 890 small urban ~~catchments basins~~ were ~~defined-delineated~~ (Fig. 2a3a). The hydrographic network linking these small ~~catchments basins~~ was defined as all the meshes draining at least an area equal to 1 ha (Fig. 2b3b). For this network, we differentiated between meshes with known geometric characteristics (widths and depths of the main ~~canals channels~~, i.e. 297 sections) and those with unknown characteristics (either natural sections or sections with unknown dimensions). ~~These meshes were given a different numerical code to apply a different parameterisation to the 1D kinematic wave model. The retention basins can be inserted in the channels network. In the drainage structure, this network is linked to a set of 106 retention basins.~~ Each retention basin is reduced to a single mesh, representing its outlet. To this mesh is assigned a height-volume-drainage law to describe the operation of the reservoir ~~and a unique identifier has been associated to each reservoir, so that their operation can be simulated differently~~ (see section 4.3).

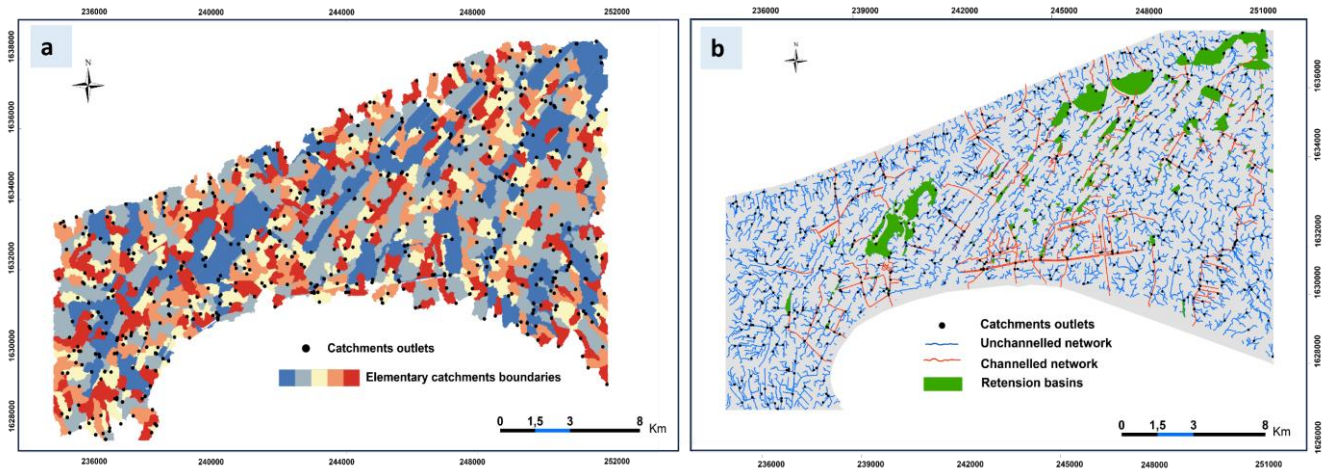


**Figure 23:** a) Partitioning of the area into small urban catchment; b) Definition of runoff transfer and storage classes

### 3.3 Application of hydrological runoff and routing model

#### 205 3.3.1 The SCS (Soil Conservation Service) runoff model

The SCS hydrological model (Ponce and Hawkins, 1996), which is often applied in small urban catchments basins (Bouvier et al., 2018; Meng et al., 2019), was used to estimate the runoff on each mesh (Maref and Seddini, 2018; Bouadila et al., 2023). This model ~~has the advantage not only of being relatively simple, capable of translating a trend towards an increase enables an increase of in~~ the runoff coefficient as a function of the cumulated rainfall, ~~but also of being supplied with charts enabling S (or its CN equivalent) with the main parameter~~ to be determined as a function of: soil type and land use, land use density, initial moisture conditions (Steenhuis et al., 1995; Huang et al., 2007).

The model's ~~adjustment~~ parameters are  $I_a$  and S (or its CN equivalent). The parameter  $I_a$  represents the initial losses before the onset of runoff (mm), and S is the maximum water retention capacity of the soil at the start of the event (mm). The model is generally applied assuming that  $I_a = 0,2.S$ , ~~and which~~ is expressed by Eq. (45):

$$215 \quad Q = \frac{(P-0,2.S)^2}{P+0,8.S} \quad P > 0,2.S ; \text{ if not } Q = 0 \quad (54)$$

where P is the total rainfall during the event (mm), Q is the runoff during the event (mm).

The dynamic formulation of this model (i.e. the temporal evolution of the flow during the event) is given by (Eq. 26), ~~derivating Eq.5 in respect with time by Gaume et al. (2004)~~:

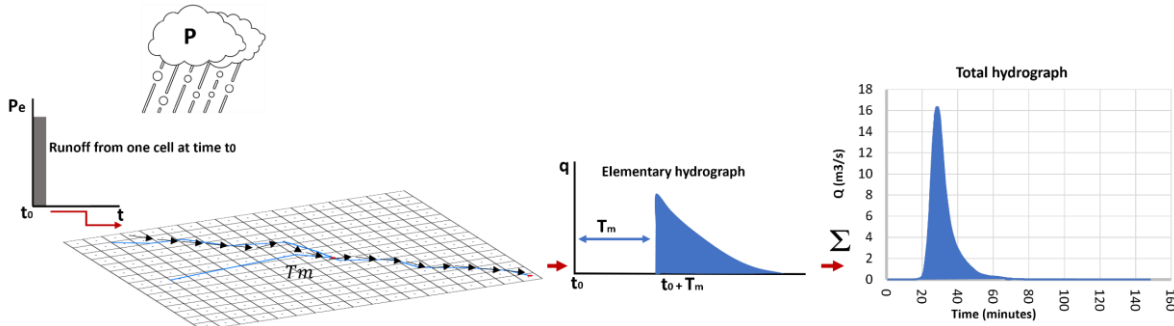
$$Pe(t) = Pb(t) \cdot \left( 2 - \frac{(P(t)-0,2.S)}{P(t)+0,8.S} \right) \left( \frac{P(t)-0,2.S}{P(t)+0,8.S} \right) \quad (62)$$

220 Where  $Pe(t)$  represents the runoff produced at time t (mm/h),  $Pb(t)$  is the intensity of the rain ~~received at time t~~ (mm/h), and  $P(t)$  the cumulative rainfall at time t, since the start of the storm (mm). S is the only model adjustment parameter. The model

is applied to each grid cell in the area ~~under consideration~~ with a time step of 5 minutes, ~~and~~ S is likely to vary spatially depending on urban conditions.

### 3.3.2 The routing model

225 ~~On~~ ~~From~~ each grid cell, the runoff provided by the SCS model is transferred to the outlet of an elementary catchment by the Lag and Route (LR) model (Fig. 34). Each ~~mesh in the entire basin~~ cell provides an ~~elementary~~ hydrograph at the outlet of the elementary catchment, and the complete hydrograph ~~is obtained~~ at the outlet of ~~each basin~~ the elementary catchment is obtained by summing the ~~elementary-cell~~ hydrographs (Tramblay et al., 2011).



230 **Figure 34:** Conceptual diagram of the Lag and route model.

The ~~cell elementary~~ hydrograph ~~provided by a mesh~~ depends on 2 variables:

- the transfer time  $T_m$  (Eq. 37) from the mesh to the basin outlet, equal to:

$$T_m = L_m/V_o \quad (73)$$

where  $L_m$  is the distance from the mesh to the outlet,  $V_o$  is the average velocity of the flow between the mesh and the outlet over the path travelled-traveled (possibly varying for each mesh)

235

- the time  $K_m$  (Eq. 48) associated with the diffusion of the flood wave during the transfer time  $T_m$ , equal to:

$$K_m = K_o \cdot T_m \quad (84)$$

where  $K_o$  is the proportionality coefficient between diffusion (lag) and translation (route) and diffusion (dimensionless).

240  $V_o$  and  $K_o$  are the 2 parameters of the LR model.

The equation of the elementary hydrograph (Eq. 59) produced by the effective rainfall  $Pe(t_0)$  obtained on each mesh at each time  $t_0$  is given by:

$$Q(t) = \frac{Pe(t_0)}{K_m} \exp\left(-\frac{t-(t_0+T_m)}{K_m}\right) A \quad \text{siif } t > t_0 + T_m \quad \text{and } Q(t) = 0 \text{ if not} \quad (95)$$

245 where  $A$  is the mesh size (here  $25\text{m}^2$ ). ~~This-The~~ LR model has the advantage of being numerically stable in respect to both the cell size and the computation time step, based on allowing fast calculation times, as used here, with cell size  $25\text{m}^2$  and time step  $5\text{mn}$ . is numerically stable and relatively easy to parameterise at the scale of the basin (Bouvier et al., 2017; Bouadila et al., 2023).

### 3.4 The propagation model in the drainage network

250 The hydraulic propagation velocity of flow propagation in the unchannelled/unchanneled network and the channelled channeled network (297 collectors) is computed simulated by the 1D Kinematic Wave (KW) hydraulic-model (Vieux and Gauer, 1994(Constantindes, 1981)). The KW model combines a conservation equation (Eq. 10):

$$\frac{\partial A}{\partial t} + \frac{\partial Q}{\partial x} = 0 \quad (10)$$

where  $Q$  is the flow rate ( $\text{m}^3/\text{s}$ ),  $A$  is the area of the wetted cross-section (in  $\text{m}^2$ ),  $x$  is the horizontal distance (m) and  $t$  is the time (s) ;

255 with a dynamic equation, used as the Manning-Strickler formula (Eq. 11) :

$$V(t) = Kr \cdot \sqrt{S_f} \cdot Rh^{2/3} \quad (11) \quad \text{using the}$$

Manning Strickler formula (Eq. 6), which takes into account the characteristics (roughness, slope and cross sectional dimensions) of each mesh of the network(Vieux and Gauer, 1994).

Its formula is given by:

$$260 \quad V(t) = Kr \cdot \sqrt{I} \quad (6)$$

where  $V(t)$  represents the flow velocity ( $\text{m}\cdot\text{s}^{-1}$ ),  $Kr$  the Manning Strickler roughness coefficient ( $\text{m}^{1/3}\cdot\text{s}^{-1}$ ),  $Rh$  (m) the hydraulic radius calculated from the channel's geometric characteristics (width  $\lambda$  and depth  $P_c$ ),  $S_f$  ( $\text{m}\cdot\text{m}^{-1}$ ) the friction slope of the land in the direction of flow,  $Rh$  (m) the hydraulic radius using :-

~~The hydraulic radius is given by Eq. (7):~~

$$265 \quad S_0 = S_f \quad (12)$$

where  $S_0$  is the channel/ground slope ( $\text{m}\cdot\text{m}^{-1}$ ).

$$Rh = \frac{S_m}{P_m} \quad (7)$$

~~Where  $S_m$  ( $\text{m}^2$ ) denotes the wetted cross section and  $P_m$  (m) the wetted perimeter.~~

~~For a rectangular cross section, these two parameters are obtained by Eq. (8) and Eq. (9):~~

$$S_m = H \cdot \lambda \quad (8)$$

$$P_m = 2 \cdot H + \lambda \quad (9)$$

To apply Eq. 11 to water flow in channels or surface runoff, it is assumed that the friction slope is equal to the bed slope (Eq. 12):

Where  $\lambda$  denotes the width of the section and  $H$  the height of water in the section. The numerical stability of the OC-KW model needs to respect the courant's condition, which leads to computation with very short times (some seconds) when using elements of small size, typically 25 m<sup>2</sup>, being more physical (Singh and De Lima, 2018). It thus requires longer computation times to calculate the mesh-to-mesh flows in the channelled and unchannelled network. The time saving is obtained by limiting the calculations to the network meshes, which means to a small number of meshes. Considering that the channels have mostly rectangular shape, the parameters of the KW model for each channelled or unchannelled cell of the drainage network are  $K_r$  the Manning-Strickler coefficient,  $\lambda$  the width of the rectangular cross-section,  $P_c$  the depth of the rectangular cross-section. The slopes of the cells can be derived from the DTM, see 4.2.

### 3.5 The water storage model in retention basins

Modelling the water storage in the retention basins is based on the principle that the retention basin is reduced to only one cell, which figures the basin outlet. This cell must have specific characteristics which must emulate the behaviour of the basin (Table 2). These characteristics are the storage (in millions of cubic meters) in the basin and the outflow rate (in cubic meters per second) at different tabulated water levels (in m) :

**Table 2: Example of a reservoir operation**

Water level (m)	Volume (10 <sup>6</sup> .m <sup>3</sup> )	Outflow (m <sup>3</sup> /s)
$Q$	$Q$	$Q$
$H_1$	$V_1$	$Q_1$
....	....	....
$H_{max}$	$V_{max}$	$Q_{max}$

where the first line is associated to the minimal storage in the basin, and the last line is associated to the maximal storage in the basin. When the maximal storage is reached, the inflow rate is added to the outflow rate. It is supposed that volumes and outflows vary linearly between 2 lines.

A specific case, with only 2 lines (1 for the minimal storage, 1 for the maximal storage), emulates a linear reservoir model for all the water levels in the basin, see 4.3.

A volume height discharge law, implemented in the Mercedes modelling module of ATHYS, provides information on the behaviour of each retention basin for different water levels. This law is tabulated and indicates, for different volumes stored in the retention basin, the corresponding height of water and the outlet flow from the reservoir. 9

Given the simple geometric shape and the type of drainage of the retention basins, this law can be summarised in 2 lines indicating the triplets heights volumes leakage rates for a zero volume in the reservoir (1<sup>st</sup> line) and for a maximum volume in the reservoir (2<sup>nd</sup> line). Between the two lines, the heights will be linearly interpolated as a function of the volume stored in the reservoir.

#### 4. Model ~~calibration~~parameterisation

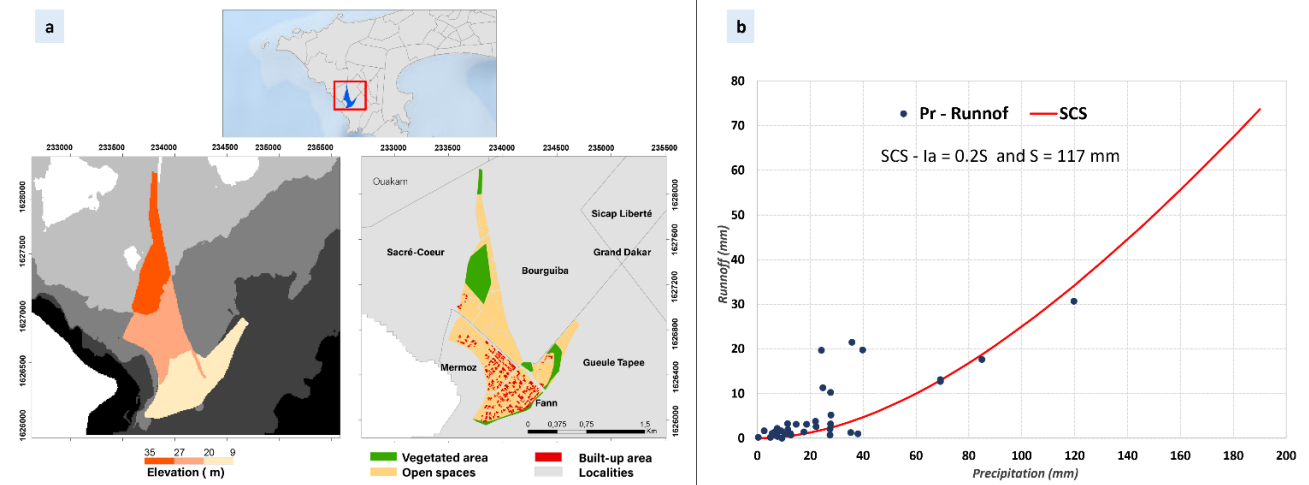
Implementing the model on the ~~scale of the entire whole~~ study area requires ~~parameterisation~~ calibration of the parameters: ~~that takes into account:~~ (i) ~~soil types and urban conditions~~  $S$  for the SCS model, (ii) the  $V_0$  and  $K_0$  ~~transfer rate of runoff~~ for the LR model, (iii)  $K_r$ ,  $\lambda$  and  $P_c$  ~~the transfer rate in the network~~ for the 1D Kinematic Wave model, (iv) the storage capacity and discharge rate at the outlet of each reservoir for the storage model, ~~and (v) the project rainfall constructed to feed the models.~~

#### 4.1 ~~Calibration~~ Parametrisation of the ~~rainfall-runoff hydrological runoff and routing~~ model

##### 4.1.1 ~~Calibration~~ Parametrisation of the SCS runoff model

To calibrate the ~~production hydrological~~ model, we first ~~estimated the infiltration rates~~ ~~measured rainfall and soil moisture~~ on the very sandy ~~\_soils often found in Dakar (Diémé, 2023), and calculated infiltration by\_~~ ~~using inverse modelling of~~ ~~inverting~~ soil moisture measurements ~~in relation to rainfall~~ (Le Bourgeois et al., 2016). Tests carried out using Hydrus 1D software (Šimůnek et al., 2016) showed that these soils were highly permeable, and capable of infiltrating rainfall in full (Diémé, 2023).

We then used hydrological data available for the city of Dakar (Fig. ~~4b5b~~) and measured in the Fann Mermoz experimental ~~basin catchment~~ by Bassel et al. (1994) and Bassel and Pépin (1995). ~~These data, collected during the two measurement campaigns, Both observed rainfall and runoff data~~ make it possible to evaluate the runoff coefficients for different rainfall events (Fig. ~~4b5b~~) in this experimental ~~catchment~~basin, where the built-up coefficient was approximately 20% (Fig. ~~4a5a~~).



320 **Figure 45:** a) Characteristics of the Fann Mermoz experimental basin; b) Relationship between rainfall and runoff (data taken from Bassel, 1996).

The estimated ~~Estimated~~ runoff coefficients are of the order of 10% for a rainfall of 40 mm, 20% for a rainfall of 78 mm, and 30% for a rainfall of 150 mm. In other words, the ~~basin's build-up~~ coefficient of the catchment is close to the runoff coefficient associated with a rainfall of 78 mm, i.e. a rainfall with a ten-year return period in Dakar (Sane et al., 2018). This is consistent with the filtering nature of the soil, as we have ~~characterised~~ characterized, which indicates that unpaved soils produce negligible runoff for most rainfall events. To obtain a runoff coefficient of 20% with a rainfall of 78mm, the value of the S parameter of the SCS model must be set to 117mm.

325 Finally, we ~~generalised~~ generalized the assumption that the building coefficient is equal to the runoff coefficient associated with a ten-year rainfall for the entire Dakar site. The ~~building build-up~~ coefficients were calculated for each urban block, as the ratio of the surface area of the buildings to the surface area of the block (Fig. 56). All the meshes within the same urban block were then assigned the value calculated for the block.

330

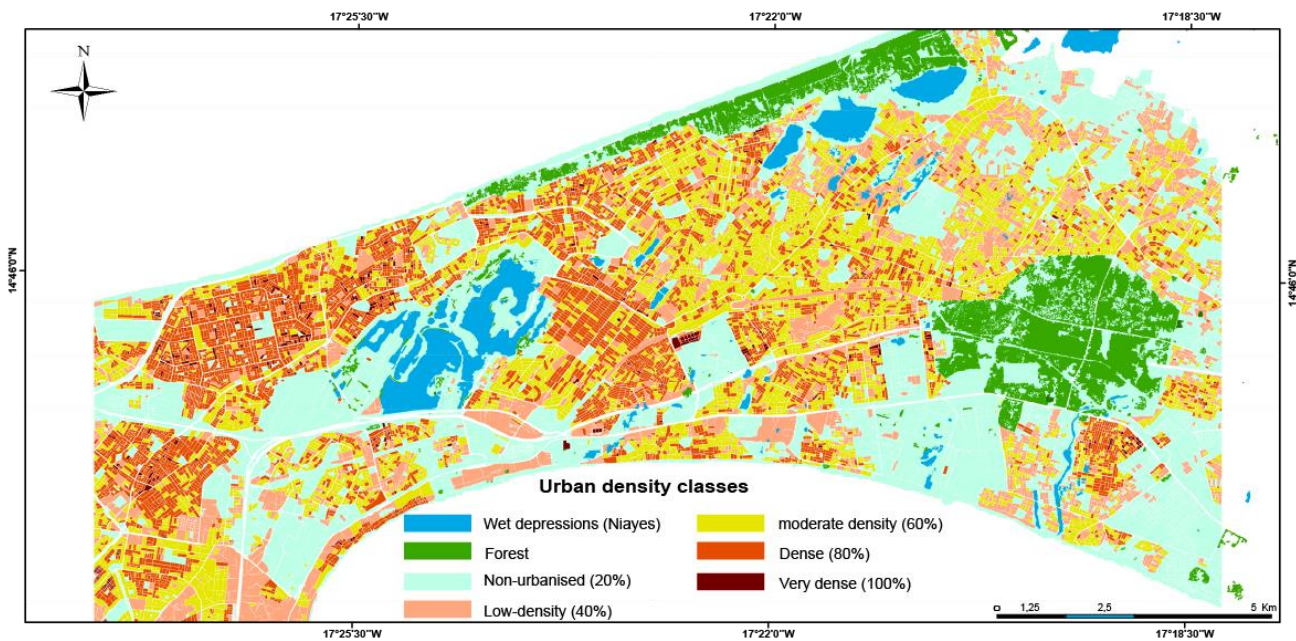


**Figure 56:** Determination of urban density classes by urban block

Finally, we calculated the values of S for different classes of building coefficient, following Eq. (130):

$$335 \quad CR = \frac{Q}{P} = \frac{(P-0.2S)^2}{P \cdot (P+0.8S)} \quad (134)$$

Where P is the height of the 10-year rainfall in 4 hours, i.e. 78 mm. The values obtained after adjusting the S parameter are shown in Table 42.

**Table 42:** Summary of values obtained for the S parameter of the SCS model

Urban density classes %	Run-off coefficient (ten-yearly)	S values
20	20	117
40	40	67
60	60	35
80	80	15
100	100	0

#### 4.1.2 Parametrisation-Calibration of the routing model

340 The Ko parameter was set at 0.7, the empirical value usually used (Bouvier et al., 2017). The Vo parameter was determined by using historical data from the Fann Mermoz experimental catchmentbasin (Bassel, 1996).



Based on the observed data of ~~In~~-this study, we considered the basin response time ( $T_r$ ) to be the same as that the lag-time  $T_r$  (between the center of gravity of the runoff and the center of gravity of the rainfall) could be estimated to be 30 mn. We considered that this lag-time should be the same as the one provided by the LR model, applied to the mesh occupying the center of gravity of the catchment basin's active zone (urbanized area). This mesh is located approximately 1.2 km from the basin outlet. The theoretical response time provided by the model is given by Eq. (~~14~~14):

$$T_r = T_m + K_m \quad (1414)$$

With  $m$  the mesh of the basin's center of gravity of the catchment, this leads to Eq. (~~15~~15):

$$T_r = 1.7 T_m = 1.7 L_m/V_o \quad (1512)$$

345 And therefore  $V_o$  is obtained using Eq. (~~13~~16):

$$V_o = 1.7 L_m/T_r \quad (1613)$$

~~Response times were estimated at an average of 30 minutes based on available rainfall runoff observations, taking into account the difference between peak rainfall and peak runoff. For a distance from the center of the basin to the basin outlet equal to 1.2 km, the calculated flow transfer velocity ( $V_o$ ) is equal to~~ Applying Eq. 16 with  $T_r = 30$  mn and  $L_m = 1.2$  km

355 ~~leads to~~  $V_o = 1.1$  m/s.

This ~~estimation parameterization~~ based on data from the experimental catchment basin was then extrapolated to the ~~scale of the whole~~ study area, considering the velocity  $V_o$  transfer rate to be uniform and equal to that obtained for the Fann-Mermoz catchment basin for all rainfall events. This approximation is justified by the fact that slopes vary little in Dakar, and are on average fairly close to those of the Fann-Mermoz catchment basin.

## 360 4.2 1D hydraulic model calibrationparametrisation

### 4.2.1 Propagation in the unchannelledunchanneled network

The unchannelledunchanneled network meshes here have been linked to both (i) the right-of-way of streets and roads which, in urbanized areas, become the transfer pathways for surface runoff (Zhang et al., 2018; Skrede et al., 2020) due to the presence of buildings, walls and other urban objects (Fig. ~~6~~7) that divert flows (Diémé et al., 2022) and (ii) the shallow natural reaches arising from non-urbanized surfaces. ~~The directions of flow that can pass through these unchannelledunchanneled meshes were defined when constructing the drainage topology (section 3.1).~~



370 **Figure 67:** Surface water drainage paths at urban street level.

The network meshes derived from streets and roads were classified into types (residential streets, primary-secondary roads, national roads, and freeways), and assigned a specific width according to their spatial footprint. This was done interactively, on-screen, by superimposing the city's roads and streets layer onto a satellite imagery background (Google Earth). The widths ( $\lambda$ ) corresponding to each category of the road were estimated on a case-by-case basis, taking considering into

375 account the alignment of the carriageway and its verges. The Figure 7-8 shows the values found (in meters) and defined using Google Earth's Earth's distance measurement tools. As there are no constraints (walls, partitions, etc.) in the propagation of natural reaches, they have been considered in the model as having infinite width.



**Figure 78:** Determining the widths of unchannelled/unchanneled transfer classes

380 With regard to About the depth of the minor bed ( $P_c$ ) associated with street and road meshes, an infinite depth has been set, so that the flow remains channelled channeled by the width of the road or street (in this case by the walls bordering the street) and considered to be null for the meshes of the natural reaches, which are very little marked in Dakar. Manning

Strickler roughness coefficients were estimated at  $50 \text{ m}^{1/3} \cdot \text{s}^{-1}$  for all street and road meshes with more or less smooth surfaces, and at  $20 \text{ m}^{1/3} \cdot \text{s}^{-1}$  for natural meshes with rough ~~surfaces~~ surfaces.

385 Slope values were calculated from the DTM, using the differences in elevation at the nodes of each mesh, in the mesh's drainage direction, then smoothed, ~~in order to~~ limit the sensitivity of the 1D Kinematic Wave model to slope variability (sometimes linked to DTM accuracy shortcomings). Smoothing was based on the difference between the altitudes of the mesh and the  $N^{\text{th}}$  mesh downstream, divided by the length of the trajectory between the mesh and the  $N^{\text{th}}$  mesh downstream. The number N of meshes used for smoothing has been set at 50 meshes. If the calculated slope is equal to 0 (or even  $<0$ ) or  
390 there is no  $N^{\text{th}}$  mesh (on the edges of the image), this slope is assigned the value 0.001 m/m. Slopes smoothed in this way range from 0.001 to 0.4 m/m, with an average of 0.007 m/m.

#### 4.2.2 ~~Calibration Parametrisation~~ of the propagation model in the ~~channelled~~ channeled network

The parameters  $\lambda$  and  $P_c$ , ~~used to calculate the hydraulic radius,~~ were set ~~on the basis of~~ based on the dimensions of the collectors for which information on their characteristics (width and depth) is available in the preliminary and detailed  
395 technical reports produced as part of PROGEP. The roughness coefficient has been uniformly set at  $50 \text{ m}^{1/3} \cdot \text{s}$ , and flows are calculated over all channel sections, taking into account the overall rectangular cross-section. The slopes applied are obtained by smoothing the DTM altitudes as indicated above.

#### 4.3 ~~Calibration Parametrisation~~ of the water storage model

All the retention basins were considered having regular shapes where the volume and the water level were proportional. They also were considered as having a linear reservoir behaviour, so that the outflow and the storage volume (or the water level) are also proportional. Thus, the volume-water level-outflow can be reduced to only 2 lines, where the upper line denotes the lowest volume, water level, and outflow in the basin, and the lower line the highest volume, water level, and outflow in the basin. For example, a basin that has  $15\,000 \text{ m}^3$  maximal volume, 1.2 m maximal water level, and  $3.90 \text{ m}^3/\text{s}$  maximal outflow will be associated with table 2.

405 ~~In the list of retention basins (106), only the retention basins built as part of the PROGEP project (84 basins) have detailed information (storage capacity, height and discharge rate), which we have extracted from the various reports produced by this project. As for the other basins whose dimensions are not known, we have assigned them, by default, characteristics based on a criterion of similarity of the shapes of their contours with those of basins whose dimensions are known, and by visually comparing them using satellite imagery from Google Earth. The 106 selected have been included in the flow modeling chain, and their operation at different water levels is simulated by a volume height flow law defined in the ATHYS Mercedes module. In the simulations, leakage flow rate has a constant value (Table 2), corresponding to the capacity of the nozzle or the drainage channel located at the reservoir outlet, at the lowest level of the reservoir bottom.~~

Table 2: Example of a reservoir operation

<u>Height Water level (m)</u>	<u>Volume (10<sup>6</sup>m<sup>3</sup>)</u>	<u>Emptying rate Outflow (m<sup>3</sup>/s)</u>
0	0	<u>3,900</u>
1,2	15 000	3,90

From this table, each value of water level or outflow corresponding to a given volume is linearly interpolated between the minimal and the maximal storage volumes.

When maximum reservoir storage value capacity is reached, the inflow entering the reservoir is fully transferred downstream as outflow. However, when there is no outlet channel, the entire volume of water is stored in the reservoir, so there is no transfer downstream.

In the list of retention basins (106), only the retention basins built as part of the PROGEP project (84 basins) have detailed information (storage capacity, maximum water level and discharge rate), which we have extracted from the various reports produced by this project. As for the other basins whose dimensions are not known, we have assigned them, by default, characteristics based on a criterion of similarity of the shapes of their contours with those of basins whose dimensions are known, and by visually comparing them using satellite imagery from Google Earth.

## 5 Modelling of the drainage overflow

### 4.45.1 Project rainfall Design storms construction

Project rainfall Design storms (Fig. 9) was were constructed to be used as input data for injected into the model and to simulate runoff discharges (Zhenyu and Olivier, 2005; Balbastre-Soldevila et al., 2019). They were constructed from the IDF curves that we calculated using the GEV law parameter values ( $\mu$ ,  $\sigma$ ,  $\epsilon$ ) established by Sane et al. (2018), for each region of Senegal. In order to obtain a reliable estimate of the distribution parameters  $\mu$ ,  $\sigma$  and  $\epsilon$  for each rainfall station, Sane et al. (2018) mixed all the data of different durations considering that the distributions of rainfall of duration  $d$  are identical to within one factor,  $\eta$ , called the scaling factor. This approach makes it possible to create a single sample of rainfall of different durations by grouping together all the maximum annual rainfall values of all durations  $d$ , after dividing each rainfall of duration  $d$  by a quantity  $d^\eta$ . Finally, they fitted a GEV distribution to this sample, with the Dakar parameters  $\mu = 28.9$  mm,  $\sigma = 12.5$  mm,  $\epsilon = 0.08$ , with  $\eta$  set to  $\eta = -0.86$ . The parameters associated with the rainfall distributions for each duration  $d$  are obtained using Eq. (14), Eq. (15) and Eq. (16):

$$\mu = \text{-----} (14)$$

$$\sigma = \text{-----} (15)$$

$$\epsilon = \epsilon \text{-----} (16)$$

440 This makes it possible to determine the maximum rainfall of duration  $d$  (1 to 24 hours) corresponding to each return period of 2 years to 100 years (Fig. 8a).

~~This~~The maximum rainfall provided by the IDF curves (table 1), ~~calculated for different return periods,~~ was ~~then~~ used to construct the ~~project rainfall~~design storms. The design ~~storm~~ rainfall model used is the double triangular rainfall model proposed in France by Desbordes and Raous (1976). ~~This form of synthetic hyetogram, in which the position of the rainfall intensity peak is centred, has the advantage of guaranteeing hydrological models' maximum efficiency in calculating hydrographs (Roux et al., 1995).~~It takes into account: (i) the total duration of the rain,  $t_3$ , whose height taken from the IDF is equal to  $P(t_3, T)$ , (ii) the period of intense rain of duration  $t_1$ , whose height  $P(t_1, T)$ , is also taken from the IDF and (iii) a period  $t_2$  (here  $\frac{t_3-t_1}{2}$  in case of a symmetric design rainfall) which constitutes a period of rain before and after the intense period. For its construction, the basic parameters to be determined are  $i_m$  (the maximum intensity before the intense period) and  $i_M$  (the maximum intensity of the peak of the intense rainfall). They ~~is~~ are calculated following Eq. (17 and 18):

$$i_m = \frac{P(t_3, T) - P(t_1, T)}{t_2} \quad (17)$$

Where  $P$  is the height of the rainfall,  $T$  is the return period,  $t_3$  is the total duration of the rainfall with a period fixed here at 4 hours, representative of the average duration of rainfall in the region,  $t_1$  is the duration of the intense rainfall, and corresponds to the time of concentration in the basin (fixed here at 1 hour due to the nature of the data from the IDF curves, which do not provide sub-hourly intensities).

The second parameter  $i_M$  is calculated following Eq. (18):

$$i_M = \frac{2P(t_1, T)}{t_1} - i_m \quad (18)$$

To build the design storm for different return periods, we selected a total duration  $t_3 = 4h$  generally observed in African convective systems (Tadesse and Anagnostou, 2010). The duration of the intense rainfall  $t_1$  must be related to the time of concentration of the catchments; we chose  $t_1 = 1h$  according to the transfer time over the largest catchments. Other attempts using 30 mn and 10 mn do not show significant differences in the flow discharges at the outlet of the catchments, whatever size they have. Based on  $i_m$  and  $i_M$ , rainfall intensities are then determined for every 5 minutes by linear interpolation between times 0 and  $t_2$ . ;  $t_2$  and  $t_2 + \frac{t_1}{2}$ ;  $t_2 + \frac{t_1}{2}$  and  $t_2 + t_1$ ;  $t_2 + t_1$  and  $t_3$ . The project rainfalls constructed with  $t_1 = 1h$  and  $t_3 = 4h$  for different return periods are shown in Figure 8b.

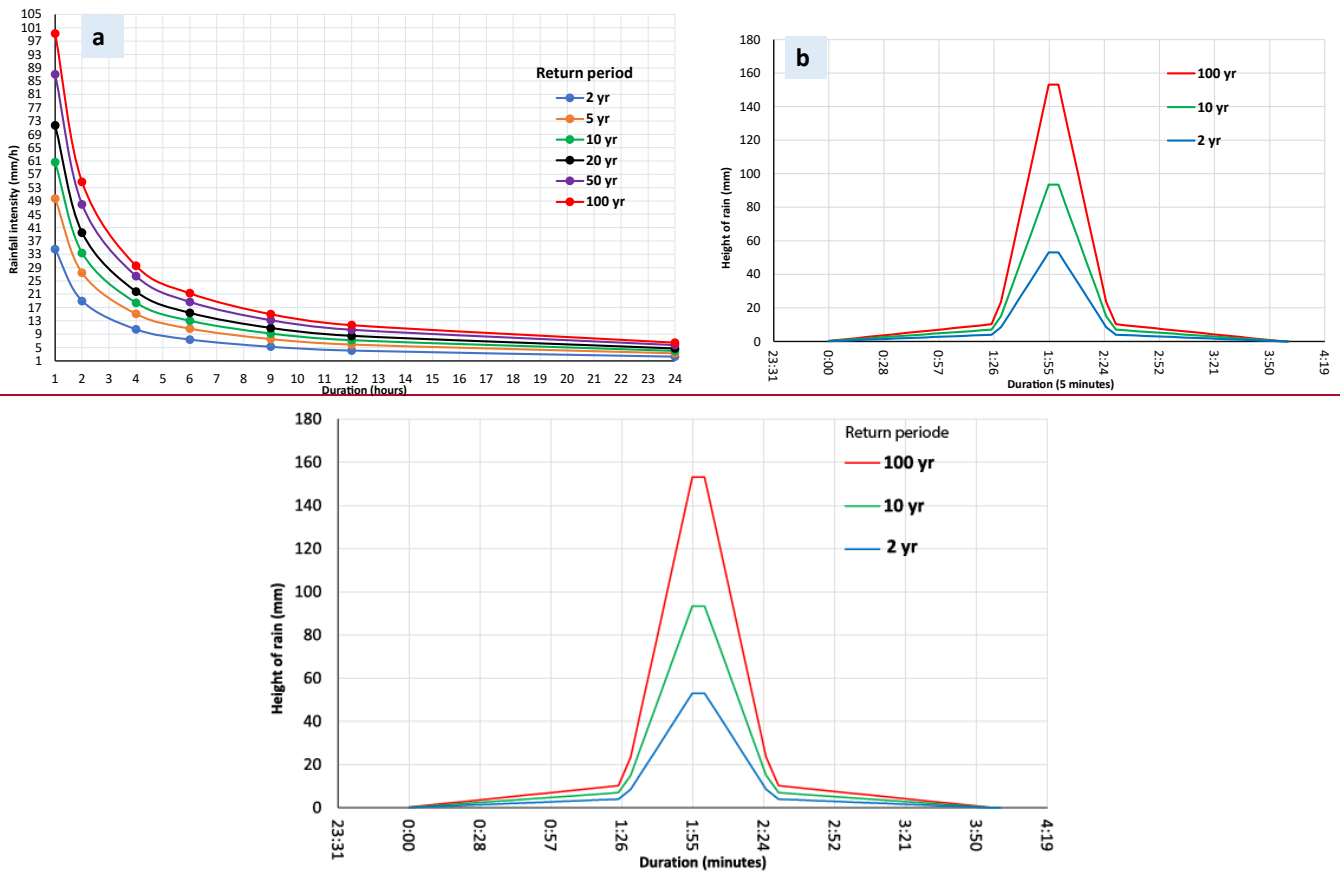


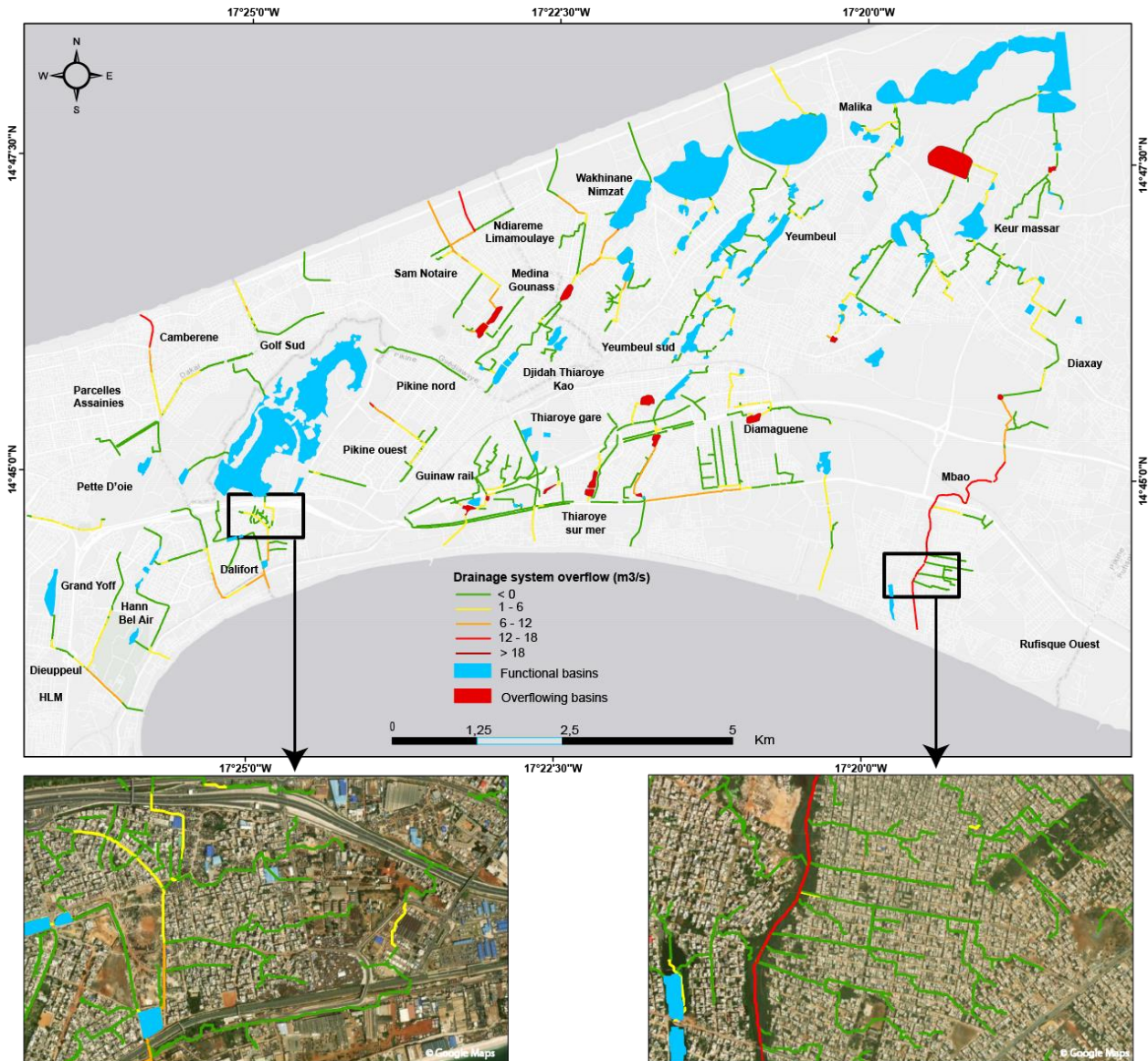
Figure 89: (a) IDF rainfall curves for Dakar calculated from the CEV parameters defined by Sané et al. (2018); (b) Construction of the project rainfall design storms for return periods of 2, 10 and 100 years with an intense period of 1 hour and 4 hours total duration.

## 5. Results and discussion

### 5.1.2 Application-Implementation to detecting network overflows

Running the simulation model provides the flows, heights and velocities in the drainage and storage networks over the course of throughout the event. The overflows from the network correspond to a positive difference between the simulated flows and the full-load capacities for the drainage network, and to a positive difference between the simulated volume and the maximum volume for the storage basins. The capacities of the drainage network were calculated by applying the Manning-Strickler formula at full load, i.e. with a head of water corresponding to the depth of the structure. The results are maps of overflows from the stormwater drainage network and retention basins at the scale of the study area. The results presented here are based on running the model with 10-year (78 mm; Fig. 910) and 100-year (128 mm; Fig. 1011) project rainfall design storm over a 4 hour period 4 hours. The simulations were carried out on the assumption that the rainfall was uniform over all the defined catchment areas. The simulations carried out show that the network records significant

overflows for rainfall with a ~~10-years~~10-year return period, with overflow levels ranging from 1-12 m<sup>3</sup>/s for some sections and ~~12- until~~ 18 m<sup>3</sup>/s for three sections. For most of the collectors that overflowed, the overflow rate varied between 1 and 6 m<sup>3</sup>/s.



485

Figure 910: Identification of network overflow points for a 10-year return period rainfall.

Beyond ~~Above~~ the ten-year rainfall frequency, the network shows widespread overflow levels. This applies to both collectors and storage basins. However, some reservoirs are still operational. The large natural depressions (the Niayes) do not overflow. Overflows are noted on a large proportion of the collectors, with thresholds sometimes exceeding  $18 \text{ m}^3/\text{s}$  in some cases. The simulations also show that the flow load has caused a large number of retention basins to overflow.

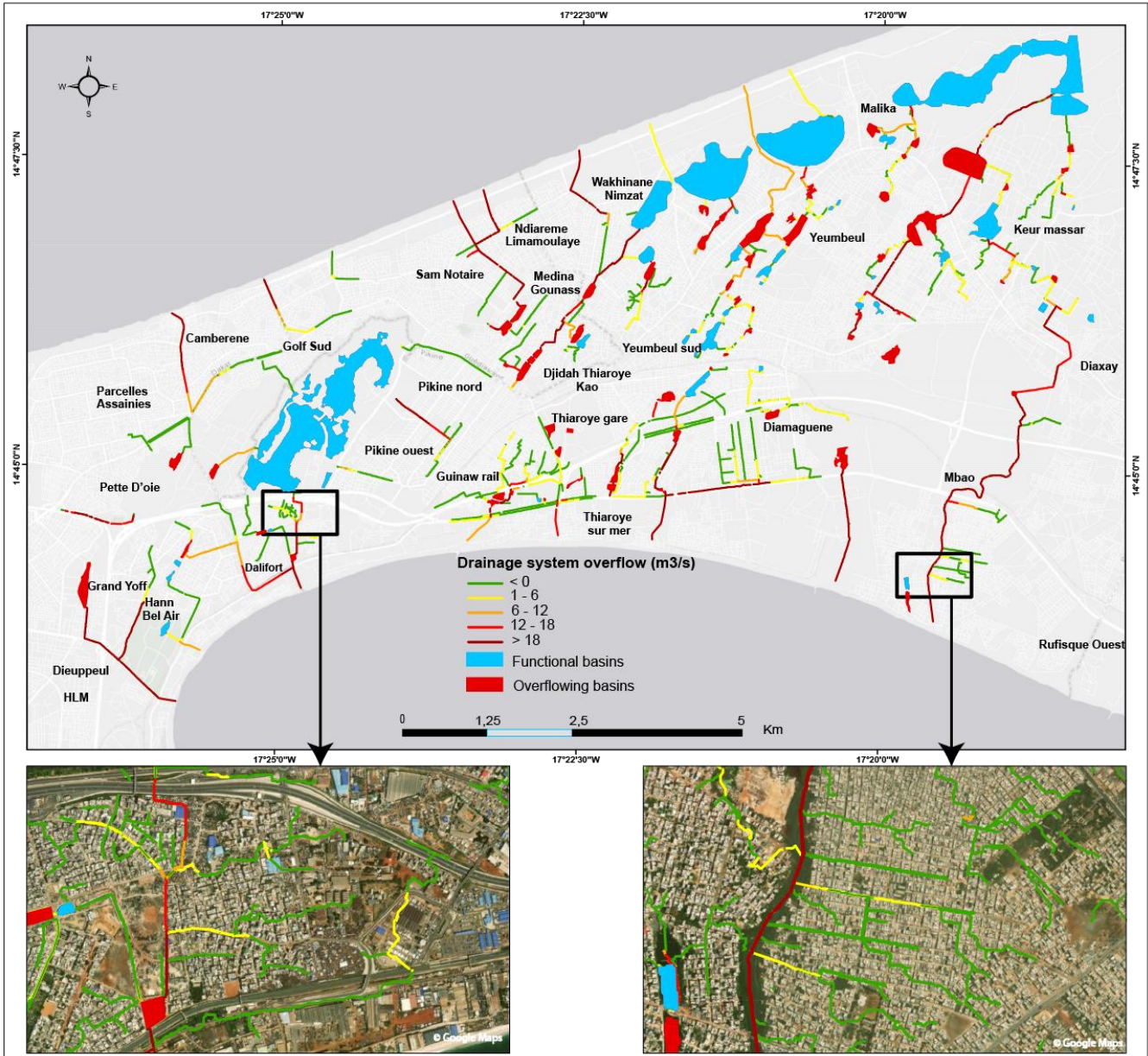


Figure 110: Identification of network overflow points for a 100-year return period rainfall.



### 5.2.3 Discussion

495 The model used in this study has the advantage of being relatively simple and is capable of covering an entire city with a fine resolution ( $5\text{m}^2$ ) and short calculation times (typically 5 minutes). This makes it a useful tool for assessing flood risk. The model is also compatible with real-time flood forecasting applications, if remote rainfall data is available. However, this study has a number of limitations. An important factor is the construction of the drainage topology based on the DTM, which has focused solely on the effects of the location of buildings, canals, and storage basins in modifying drainage directions. To  
500 obtain a more detailed view, the analysis should be extended to include other urban objects that influence the trajectories of surface runoff flows. Future work will focus on lidar data (currently being compiled for the Dakar region), which provides more detail than DTM on urban micro-objects and could thus be used to refine the reconstruction of induced drainage directions.

The other limitation of this work relates to the availability of the data (hydrological, hydrometric, or piezometric) required to  
505 ~~parameterise-calibrate~~ the hydrological runoff-routing models (SCS-LR) applied to this drainage topology ~~in order to~~ calculate flows. ~~In this study, The parameterisation-the calibration~~ of the SCS runoff model was based on the hypothesis ~~that we established, using from~~ short series of data from the Fann Mermoz experimental basin, by considering that the ten-year runoff coefficient is equal to the building coefficient. Although this simplification may be acceptable for the case of Dakar, where soils are generally sandy and very permeable (Diémé, 2023), new data must be produced to verify the hypothesis. In  
510 other cities where the soils are less permeable, direct (Kelleners et al., 2005) or indirect (Galagedara et al., 2003) infiltration measurements on several representative sites should be used as a basis for determining the contribution of these soils to surface runoff. ~~- A particular constraint is the influence of the rising water table in Dakar (Faye et al., 2019), which must be taken into account in the flow generation model. One possible solution is to obtain piezometric data giving the water table level and reduce the S parameter of the SCS model on the meshes corresponding to outcrops of the water table. The rainfall data used as input to the model was applied on the assumption that the rainfall was uniform over all the defined catchment areas. Such a hypothesis does not account for the areal reduction factor, but can be adopted because most of the catchments (i.e. 94%) have small areas, less than  $2\text{ km}^2$ . The largest catchment areas account for 4% ( $2\text{ to }6\text{ km}^2$ ) and 2% ( $6\text{ to }12\text{ km}^2$ ) out of the 890 catchment outlets which have been considered. Also, to take better account of the extreme precipitation regime, it would be interesting, instead of stationary IDF curves (used in this study), to explore non-stationary statistical~~  
515 ~~methods for determining IDF curves (Chagnaud et al., 2021) that incorporate the uncertainties associated with climate change. Likewise, a good integration of the spatial variability of precipitation is necessary for more accurate surface water runoff simulation. Alternative and innovative methods based on rainfall estimation using microwave links from cellular communication networks (Turko et al., 2021; Djibo et al., 2023) are currently being tested in African cities where the coverage of rainfall measurement stations is poor.~~

525 ~~About The~~the LR routing model, ~~it~~ was calibrated by considering the transfer velocity ( $V_0$ ), calculated on the Fann Mermoz experimental basin, as uniform over the entire study area. The slope conditions, which vary little in the study area, allow us

to retain this approximation. It is clear that the ~~parameterisation-calibration~~ of both the SCS-LR runoff-routing models needs to be improved using new experimental data, which is relatively rare in African cities. This should motivate the setting up of new experimental sites, in order to better estimate the parameters of the flow calculation models.

530 ~~Additionally, One-one~~ of the ~~improvements to be made to the model concerns~~ ~~ways in which the model has been improved is~~  
~~in~~ the calculation of the slopes used by the ~~OC-KW~~ hydraulic model to ensure the propagation of flows in the ~~channelled~~  
~~channeled~~ and ~~unchannelled~~~~unchanneled~~ network. A simplification has been applied, involving smoothing to reduce the  
sensitivity of the ~~OC-KW~~ model to irregular variations in the slope of the terrain, sometimes linked to a mistake in the DTM.  
The availability of lidar data in the study area will enable us to compare the model's performance using more accurate  
535 slopes. Similarly, the congestion of collectors (household waste, silting, etc.) can be incorporated into the hydraulic model.  
This could be taken into account by reducing the cross-section of the collector, even if information on this congestion is  
difficult to obtain. ~~A particular constraint is the influence of the rising water table in Dakar (Faye et al., 2019), which must~~  
~~be taken into account in the hydrological production model. One possible solution is to obtain piezometric data giving the~~  
~~water table level and reduce the S parameter of the SCS model on the meshes corresponding to outcrops of the water table.~~  
540 ~~Also, to take better account of the extreme precipitation regime, it would be interesting, instead of stationary DFIs (used in~~  
~~this study), to explore non-stationary statistical methods for determining DFIs (Chagnaud et al., 2021) that incorporate the~~  
~~uncertainties associated with climate change.~~

Finally, validating the results of the model simulations is one of the major perspectives of this study. ~~As things stand at~~  
~~present, it was not possible to get the necessary data for the validation of the method, which means on the one hand sub-daily~~  
545 ~~rainfall data, and on the other hand flood maps for the recent events that occurred in Dakar. The imminent installation of a~~  
~~rain gauge radar in Dakar could help to facilitate this. Flood maps could be obtained by exploring citizen science tools(Sy et~~  
~~al., 2020). This could be done by~~ using information on feedback, recent flooding situations, and data on the intensity of  
rainfall events that cause flooding ~~as applied to Bamako (Mali). An identical approach has already been proposed for the city~~  
~~of Bamako (Mali) by (Chahinian et al., (2023), or order a high-precision satellite image to map out flooded areas. The aim is~~  
550 ~~to compare simulations of flood situations that have already occurred with flood maps or feedback data.(Sy et al., 2020)~~  
Validation of the method would enable it to be extended to other towns and cities, thereby ensuring sound planning  
decisions.

## 6 Conclusions

A fine-scale simulation model of runoff over an entire urban area and an assessment of the response of the storm drainage  
555 network (canals and retention basins) to different rainfall events has been developed. It is based on a preliminary  
reconstruction of the drainage directions modified by ~~urbanisation-urbanization~~ and the implementation of combined  
hydrological and 1D hydraulic models calibrated to the city's urban conditions.

The results obtained are overflow maps for the city's drainage network for rainfall intensities of different return periods. The representation of overflow points is associated here with one-dimensional modelling, but is still sufficiently informative to guide the deployment of emergency services on the ground, or to initiate action at strategic locations: assessment of the effectiveness of planned developments, tests of different rainfall and ~~urbanisation~~ urbanization scenarios, detection of overflows in near-real time with remote rainfall data. In addition, the model also provides boundary conditions for applying 2D hydraulic models to determine locally the propagation of overflows from stormwater drainage network over limited areas. Future work will focus on improving the availability of data to facilitate the assessment of simulation uncertainties and validate the overflow results. Indeed, one of the challenges of urban hydrology in African cities is to set up urban databases that are essential for conducting relevant studies and for better ~~characterising~~ characterizing and forecasting floods.

### **Data Availability**

The data used in this article are available from the first author, LPM Diémé, upon reasonable request.

### 570 **Author contribution**

~~LPMD has conceived and designed the analysis. CB has implemented the tools codes on ATHYS. AS has provided the data and AB has contributed to the data analysis.~~ LPMD conceptualized and performed the draft preparation. CB implemented the codes on ATHYS software. AB contributed to data analysis. AS has provided Geographic datasets. LPMD, CB, and AB developed the methodology, provided the simulation and details about it. All authors were involved in reviewing and editing the paper.

### 575 **Competing interests**

The authors report no conflicts of interest.

### **Acknowledgements**

This article was produced with the support of the Water Cycle and Climate Change (CECC) 2021-2025 project, co-funded by IRD and AFD. The authors would also like to thank the technical structures that agreed to make the data used in this article available.

## References

- Agonafir, C., Lakhankar, T., Khanbilvardi, R., Krakauer, N., Radell, D., and Devineni, N.: A review of recent advances in urban flood research, *Water Secur.*, 19, 100141, <https://doi.org/10.1016/j.wasec.2023.100141>, 2023.
- ANSD (Agence Nationale de la Statistique et de la démographie): Recensement Général de la Population et de l'Habitat, de l'Agriculture et de l'Élevage (RGPHAE), rapport définitif, 418 pp., <https://anads.ansd.sn/index.php/catalog/51/related-materials> (last access: 30 October 2023), 2013.
- Balbastre-Soldevila, García-Bartual, and Andrés-Doménech: A Comparison of Design Storms for Urban Drainage System Applications, *Water*, 11, 757, <https://doi.org/10.3390/w11040757>, 2019.
- Barau, A. and Wada, A. S.: Do-It-Yourself Flood Risk Adaptation Strategies in the Neighborhoods of Kano City, Nigeria, in: *African Handbook of Climate Change Adaptation*, edited by: Ogue, N., Ayal, D., Adeleke, L., and da Silva, I., Springer International Publishing, Cham, 1353–1380, [https://doi.org/10.1007/978-3-030-45106-6\\_190](https://doi.org/10.1007/978-3-030-45106-6_190), 2021.
- 585
- Bassel, M.: Eaux et environnement à Dakar-Pluies, ruissellement, pollution et évacuation des eaux. Contribution à l'étude des problèmes d'environnement liés aux eaux dans la région de Dakar, PhD thesis, Université Cheikh Anta Diop de Dakar, Département de Géographie, 244 pp., <https://www.documentation.ird.fr/hor/fdi:010012652> (last access: 20 October 2023), 1996.
- 590
- Bassel, M., and Pépin, Y.: Pluies, ruissellement, évacuation et qualité des eaux sur le bassin versant de Mermoz-Fann: Contribution à l'étude des problèmes d'environnement liés aux eaux dans la région de Dakar, rapport de campagne, ORSTOM, 59 pp., <https://www.documentation.ird.fr/hor/fdi:010010028> (last access: 20 October 2023), 1995.
- Bassel, M., Pépin, Y., and Thiébaux, J. P.: Rapport de campagne: Bassin urbain de Dakar, ORSTOM, 55 pp., <https://www.documentation.ird.fr/hor/fdi:010020660> (last access: 27 October 2023), 1994.
- 600
- Bentivoglio, R., Isufi, E., Jonkman, S. N., and Taormina, R.: Deep learning methods for flood mapping: a review of existing applications and future research directions, *Hydrol. Earth Syst. Sci.*, 26, 4345–4378, <https://doi.org/10.5194/hess-26-4345-2022>, 2022.
- Bichet, A. and Diedhiou, A.: West African Sahel has become wetter during the last 30 years, but dry spells are shorter and more frequent, *Clim. Res.*, 75, 155–162, <https://doi.org/10.3354/cr01515>, 2018.
- 605
- Bodian, A.: Caractérisation de la variabilité temporelle récente des précipitations annuelles au Sénégal (Afrique de l'Ouest), *Géographie Phys. Environ. Physio-Géo*, 8, <https://doi.org/10.4000/physio-geo.4243>, 2014.
- Bottazzi, P., Winkler, M. S., Boillat, S., Diagne, A., Maman Chabi Sika, M., Kpangon, A., Faye, S., and Speranza, C. I.: Measuring Subjective Flood Resilience in Suburban Dakar: A Before–After Evaluation of the “Live with Water” Project, *Sustainability*, 10, 2135, <https://doi.org/10.3390/su10072135>, 2018.
- 610
- Bouadila, A., Bouizrou, I., Aqnouy, M., En-nagre, K., El Yousfi, Y., Khafouri, A., Hilal, I., Abdelrahman, K., Benaabidate, L., Abu-Alam, T., Stitou El Messari, J. E., and Abioui, M.: Streamflow Simulation in Semiarid Data-Scarce Regions: A

- Comparative Study of Distributed and Lumped Models at Aguenza Watershed (Morocco), *Water*, 15, 1602, <https://doi.org/10.3390/w15081602>, 2023.
- 615 Bouvier, C., Chahinian, N., Adamovic, M., Cassé, C., Crespy, A., Crès, A., and Alcoba, M.: Large-Scale GIS-Based Urban Flood Modelling: A Case Study on the City of Ouagadougou, in: *Advances in Hydroinformatics, SimHydro2017*, Sophia-Antipolis, France, 703–717, [https://doi.org/10.1007/978-981-10-7218-5\\_50](https://doi.org/10.1007/978-981-10-7218-5_50), 2017.
- Bouvier, C., Bouchenaki, L., and Tramblay, Y.: Comparison of SCS and Green-Ampt Distributed Models for Flood Modelling in a Small Cultivated Catchment in Senegal, *Geosciences*, 8, 122, <https://doi.org/10.3390/geosciences8040122>, 2018.
- 620 Bulti, D. T. and Abebe, B. G.: A review of flood modeling methods for urban pluvial flood application, *Model. Earth Syst. Environ.*, 6, 1293–1302, <https://doi.org/10.1007/s40808-020-00803-z>, 2020.
- Chagnaud, G., Panthou, G., Vischel, T., Blanchet, J., and Lebel, T.: A unified statistical framework for detecting trends in multi-timescale precipitation extremes: application to non-stationary intensity-duration-frequency curves, *Theor. Appl. Climatol.*, 145, 839–860, <https://doi.org/10.1007/s00704-021-03650-9>, 2021.
- 625 Chagnaud, G., Panthou, G., Vischel, T., and Lebel, T.: A synthetic view of rainfall intensification in the West African Sahel, *Environ. Res. Lett.*, 17, 044005, <https://doi.org/10.1088/1748-9326/ac4a9c>, 2022.
- Chahinian, N., Alcoba, M., Dembélé, N. D. J., Cazenave, F., and Bouvier, C.: Evaluation of an early flood warning system in Bamako (Mali): Lessons learned from the flood of May 2019, *J. Flood Risk Manag.*, <https://doi.org/10.1111/jfr3.12878>, 630 2023.
- Chen, Y., Zhou, H., Zhang, H., Du, G., and Zhou, J.: Urban flood risk warning under rapid urbanization, *Environ. Res.*, 139, 3–10, <https://doi.org/10.1016/j.envres.2015.02.028>, 2015.
- [Constantindes, C. A.: Numerical techniques for a two-dimensional kinematic overland flow model., \*Water SA\*, 7, 234–248, 1981.](#)
- 635 Costabile, P., Costanzo, C., De Lorenzo, G., and Macchione, F.: Is local flood hazard assessment in urban areas significantly influenced by the physical complexity of the hydrodynamic inundation model?, *J. Hydrol.*, 580, 124231, <https://doi.org/10.1016/j.jhydrol.2019.124231>, 2020.
- Coulibaly, G., Leye, B., Tazen, F., Mounirou, L. A., and Karambiri, H.: Urban Flood Modeling Using 2D Shallow-Water Equations in Ouagadougou, Burkina Faso, *Water*, 12, 2120, <https://doi.org/10.3390/w12082120>, 2020.
- 640 Darabi, H., Choubin, B., Rahmati, O., Torabi Haghighi, A., Pradhan, B., and Kløve, B.: Urban flood risk mapping using the GARP and QUEST models: A comparative study of machine learning techniques, *J. Hydrol.*, 569, 142–154, <https://doi.org/10.1016/j.jhydrol.2018.12.002>, 2019.
- Dehotin, J., Chazelle, B., Laverne, G., Hasnaoui, A., Lambert, L., Breil, P., and Braud, I.: Mise en œuvre de la méthode de cartographie du ruissellement IRIP pour l’analyse des risques liés aux écoulements sur l’infrastructure ferroviaire, *Houille Blanche*, 101, 56–64, <https://doi.org/10.1051/lhb/20150069>, 2015.
- 645

- Desbordes, M. and Raous, P.: Un exemple de l'intérêt des études de sensibilité des modèles hydrologiques, *Houille Blanche*, 62, 37–43, <https://doi.org/10.1051/lhb/1976004>, 1976.
- DHI (Danish Hydraulic Institute): Mike Flood 1D-2D and 1D-3D Modelling - user manual, 154 pp., [https://manuals.mikepoweredbydhi.help/2021/Water\\_Resources/MIKE\\_FLOOD\\_UserManual.pdf](https://manuals.mikepoweredbydhi.help/2021/Water_Resources/MIKE_FLOOD_UserManual.pdf) (last access: 17 October 2023), 2021.
- Diémé, L. P.: Système de surveillance des inondations à l'échelle de l'agglomération de Dakar, PhD thesis, Université Gaston-Berger, Département de géographie, 177 pp., <https://doi.org/10.13140/RG.2.2.19319.09121> (last access: 29 October 2023), 2023.
- Diémé, L. P., Bouvier, C., Bodian, A., and Sidibé, A.: Construction de la topologie de drainage à fine résolution spatiale en milieu urbain: exemple de l'agglomération de Dakar (Sénégal), *LHB*, 108, 2061313, <https://doi.org/doi.org/10.1080/27678490.2022.2061313>, 2022.
- Diop, L., Bodian, A., and Diallo, D.: Spatiotemporal Trend Analysis of the Mean Annual Rainfall in Senegal, *Eur. Sci. J. ESJ*, 12, 231–231, <https://doi.org/10.19044/esj.2016.v12n12p231>, 2016.
- Diop, M. S.: Les capacités adaptatives des communautés de la périphérie de Dakar face aux inondations, PhD thesis, Université Paris Saclay (COmUE), 354 pp., <https://tel.archives-ouvertes.fr/tel-02415826>, 2019.
- Faye, S. C., Diongue, M. L., Pouye, A., Gaye, C. B., Travi, Y., Wohnlich, S., Faye, S., and Taylor, R. G.: Tracing natural groundwater recharge to the Thiaroye aquifer of Dakar, Senegal, *Hydrogeol. J.*, 27, 1067–1080, <https://doi.org/10.1007/s10040-018-01923-8>, 2019.
- Gaisie, E. and Cobbinah, P. B.: Planning for context-based climate adaptation: Flood management inquiry in Accra, *Environ. Sci. Policy*, 141, 97–108, <https://doi.org/10.1016/j.envsci.2023.01.002>, 2023.
- Galagedara, L. W., Parkin, G. W., and Redman, J. D.: An analysis of the ground-penetrating radar direct ground wave method for soil water content measurement, *Hydrol. Process.*, 17, 3615–3628, 2003.
- Gaume, E., Livet, M., Desbordes, M., and Villeneuve, J. P.: Hydrological analysis of the river Aude, France, flash flood on 12 and 13 November 1999, *J. Hydrol.*, 286, 135–154, <https://doi.org/10.1016/j.jhydrol.2003.09.015>, 2004.
- Goldsmith, P. D., Gunjal, K., and Ndarishikanye, B.: Rural–urban migration and agricultural productivity: the case of Senegal, *Agric. Econ.*, 31, 33–45, <https://doi.org/10.1111/j.1574-0862.2004.tb00220.x>, 2004.
- Henonin, J., Russo, B., Mark, O., and Gourbesville, P.: Real-time urban flood forecasting and modelling – a state of the art, *J. Hydroinformatics*, 15, 717–736, <https://doi.org/10.2166/hydro.2013.132>, 2013.
- Huang, M., Gallichand, J., Dong, C., Wang, Z., and Shao, M.: Use of soil moisture data and curve number method for estimating runoff in the Loess Plateau of China, *Hydrol. Process.*, 21, 1471–1481, <https://doi.org/10.1002/hyp.6312>, 2007.
- Hungerford, H., Smiley, S., Blair, T., Beutler, S., Bowers, N., and Cadet, E.: Coping with Floods in Pikine, Senegal: An Exploration of Household Impacts and Prevention Efforts, *Urban Sci.*, 3, 54, <https://doi.org/10.3390/urbansci3020054>, 2019.

- 680 Kelleners, T. J., Robinson, D. A., Shouse, P. J., Ayars, J. E., and Skaggs, T. H.: Frequency dependence of the complex permittivity and its impact on dielectric sensor calibration in soils, *Soil Sci. Soc. Am. J.*, 69, 67–76, 2005.
- Klutse, N. A. B., Quagraine, K. A., Nkrumah, F., Quagraine, K. T., Berkoh-Oforiwaa, R., Dzrobi, J. F., and Sylla, M. B.: The Climatic Analysis of Summer Monsoon Extreme Precipitation Events over West Africa in CMIP6 Simulations, *Earth Syst. Environ.*, 5, 25–41, <https://doi.org/10.1007/s41748-021-00203-y>, 2021.
- 685 Kreibich, H., Di Baldassarre, G., Vorogushyn, S., Aerts, J. C. J. H., Apel, H., Aronica, G. T., Arnbjerg-Nielsen, K., Bouwer, L. M., Bubeck, P., Caloiero, T., Chinh, D. T., Cortès, M., Gain, A. K., Giampá, V., Kuhlicke, C., Kundzewicz, Z. W., Llasat, M. C., Mård, J., Matczak, P., Mazzoleni, M., Molinari, D., Dung, N. V., Petrucci, O., Schröter, K., Slager, K., Thielen, A. H., Ward, P. J., and Merz, B.: Adaptation to flood risk: Results of international paired flood event studies, *Earths Future*, 5, 953–965, <https://doi.org/10.1002/2017EF000606>, 2017.
- 690 Le Bourgeois, O., Bouvier, C., Brunet, P., and Ayral, P.-A.: Inverse modeling of soil water content to estimate the hydraulic properties of a shallow soil and the associated weathered bedrock, *J. Hydrol.*, 541, 116–126, <https://doi.org/10.1016/j.jhydrol.2016.01.067>, 2016.
- Lericollais, A. and Roquet, D.: Croissance de la population et dynamique du peuplement au Sénégal depuis l'indépendance, *Espace Popul. Sociétés*, 17, 93–106, <https://doi.org/10.3406/espos.1999.1872>, 1999.
- 695 ~~Lessault, D. and Imbert, C.: Mobilité résidentielle et dynamique récente du peuplement urbain à Dakar (Sénégal), *Cybergeo Eur. J. Geogr.*, <https://doi.org/10.4000/cybergeo.26146>, 2013.~~
- Li, G., Zhao, H., Liu, C., Wang, J., and Yang, F.: City Flood Disaster Scenario Simulation Based on 1D–2D Coupled Rain–Flood Model, *Water*, 14, 3548, <https://doi.org/10.3390/w14213548>, 2022.
- 700 ~~Magny, G. C. de, Thiaw, W., Kumar, V., Manga, N. M., Diop, B. M., Gueye, L., Kamara, M., Roche, B., Murtugudde, R., and Colwell, R. R.: Cholera Outbreak in Senegal in 2005: Was Climate a Factor?, *PLOS ONE*, 7, e44577, <https://doi.org/10.1371/journal.pone.0044577>, 2012.~~
- Maref, N. and Seddini, A.: Modeling of flood generation in semi-arid catchment using a spatially distributed model: case of study Wadi Mekerra catchment (Northwest Algeria), *Arab. J. Geosci.*, 11, 116, <https://doi.org/10.1007/s12517-018-3461-2>, 2018.
- 705 Mark, O., Weesakul, S., Apirumanekul, C., Aroonnet, S., and Djordjevic, S.: Potential and limitations of 1D modelling of urban flooding, *J. Hydrol.*, 299, 284–299, [https://doi.org/10.1016/S0022-1694\(04\)00373-7](https://doi.org/10.1016/S0022-1694(04)00373-7), 2004.
- Martínez, C., Sanchez, A., Toloh, B., and Vojinovic, Z.: Multi-objective Evaluation of Urban Drainage Networks Using a 1D/2D Flood Inundation Model, *Water Resour. Manag.*, 32, 4329–4343, <https://doi.org/10.1007/s11269-018-2054-x>, 2018.
- 710 Mashi, S. A., Inkani, A. I., Obaro, O., and Asanarimam, A. S.: Community perception, response and adaptation strategies towards flood risk in a traditional African city, *Nat. Hazards*, 103, 1727–1759, <https://doi.org/10.1007/s11069-020-04052-2>, 2020.

- Meng, X., Zhang, M., Wen, J., Du, S., Xu, H., Wang, L., and Yang, Y.: A Simple GIS-Based Model for Urban Rainstorm Inundation Simulation, *Sustainability*, 11, 2830, <https://doi.org/10.3390/su11102830>, 2019.
- 715 Miller, J., Vischel, T., Fowe, T., Panthou, G., Wilcox, C., Taylor, C. M., Visman, E., Coulibaly, G., Gonzalez, P., Body, R., Vesuviano, G., Bouvier, C., Chahinian, N., and Cazenave, F.: A modelling-chain linking climate science and decision-makers for future urban flood management in West Africa, *Reg. Environ. Change*, 22, 93, <https://doi.org/10.1007/s10113-022-01943-x>, 2022a.
- 720 Miller, J., Taylor, C., Guichard, F., Peyrillé, P., Vischel, T., Fowe, T., Panthou, G., Visman, E., Bologo, M., Traore, K., Coulibaly, G., Chapelon, N., Beucher, F., Rowell, D. P., and Parker, D. J.: High-impact weather and urban flooding in the West African Sahel – A multidisciplinary case study of the 2009 event in Ouagadougou, *Weather Clim. Extrem.*, 36, 100462, <https://doi.org/10.1016/j.wace.2022.100462>, 2022b.
- Mosavi, A., Ozturk, P., and Chau, K.: Flood Prediction Using Machine Learning Models: Literature Review, *Water*, 10, 1536, <https://doi.org/10.3390/w10111536>, 2018.
- 725 Moulds, S., Buytaert, W., Templeton, M. R., and Kanu, I.: Modeling the Impacts of Urban Flood Risk Management on Social Inequality, *Water Resour. Res.*, 57, e2020WR029024, <https://doi.org/10.1029/2020WR029024>, 2021.
- Ndiaye, I.: Étalement urbain et différenciation sociospatiale à Dakar (Sénégal), *Cah. Géographie Qué.*, 59, 47–69, <https://doi.org/10.7202/1034348ar>, 2015.
- Nicholson, S. E., Some, B., and Kone, B.: An Analysis of Recent Rainfall Conditions in West Africa, Including the Rainy  
730 Seasons of the 1997 El Niño and the 1998 La Niña Years, *J. Clim.*, 13, 2628–2640, [https://doi.org/10.1175/1520-0442\(2000\)013<2628:AAORRC>2.0.CO;2](https://doi.org/10.1175/1520-0442(2000)013<2628:AAORRC>2.0.CO;2), 2000.
- Nkrumah, F., Vischel, T., Panthou, G., Klutse, N. A. B., Adukpo, D. C., and Diedhiou, A.: Recent Trends in the Daily Rainfall Regime in Southern West Africa, *Atmosphere*, 10, 741, <https://doi.org/10.3390/atmos10120741>, 2019.
- Nkwunonwo, U. C., Whitworth, M., and Baily, B.: A review of the current status of flood modelling for urban flood risk  
735 management in the developing countries, *Sci. Afr.*, 7, e00269, <https://doi.org/10.1016/j.sciaf.2020.e00269>, 2020.
- Nouaceur, Z.: La reprise des pluies et la recrudescence des inondations en Afrique de l’Ouest sahélienne, *Physio-Géo Géographie Phys. Environ.*, 89–109, <https://doi.org/10.4000/physio-geo.10966>, 2020.
- Panthou, G., Lebel, T., Vischel, T., Quantin, G., Sane, Y., Ba, A., Ndiaye, O., Diongue-Niang, A., and Diopkane, M.:  
740 Rainfall intensification in tropical semi-arid regions: the Sahelian case, *Environ. Res. Lett.*, 13, 064013, <https://doi.org/10.1088/1748-9326/aac334>, 2018.
- Parvin, F., Ali, S. A., Calka, B., Bielecka, E., Linh, N. T. T., and Pham, Q. B.: Urban flood vulnerability assessment in a densely urbanized city using multi-factor analysis and machine learning algorithms, *Theor. Appl. Climatol.*, 149, 639–659, <https://doi.org/10.1007/s00704-022-04068-7>, 2022.
- 745 Pla, G., Crippa, J., Djerboua, A., Dobricean, O., Dongar, F., Eugene, A., and Raymond, M.: ESPADA : un outil pour la gestion en temps réel des crues éclaircies urbaines en pleine modernisation, *Houille Blanche*, 105, 57–66, <https://doi.org/10.1051/lhb/2019027>, 2019.



- Ponce, V. M. and Hawkins, R. H.: Runoff curve number: Has it reached maturity?, *J. Hydrol. Eng.*, 1, 11–19, [https://doi.org/10.1061/\(ASCE\)1084-0699\(1996\)1:1\(11\)](https://doi.org/10.1061/(ASCE)1084-0699(1996)1:1(11)), 1996.
- 750 Pons, F., Delgado, J., Guéro, P., Berthier, E., and Ile-de-France, C.: Exzeco: a gis and dem based method for predetermination of flood risk related to direct runoff and flash floods, 9th Int. Conf. Hydroinformatics HIC 2010 Tianjin CHINA, 2063–2070, 2010.
- Rabori, A. M. and Ghazavi, R.: Urban Flood Estimation and Evaluation of the Performance of an Urban Drainage System in a Semi-Arid Urban Area Using SWMM, *Water Environ. Res.*, 90, 2075–2082, <https://doi.org/10.2175/106143017X15131012188213>, 2018.
- 755 Rosenzweig, B. R., Herreros Cantis, P., Kim, Y., Cohn, A., Grove, K., Brock, J., Yesuf, J., Mistry, P., Welty, C., McPhearson, T., Sauer, J., and Chang, H.: The Value of Urban Flood Modeling, *Earths Future*, 9, e2020EF001739, <https://doi.org/10.1029/2020EF001739>, 2021.
- ~~Roux, C., Guillon, A., and Comblez, A.: Space time heterogeneities of rainfalls on runoff over urban catchments, *Water Sci. Technol.*, 32, 209–215, <https://doi.org/10.2166/wst.1995.0047.1995>.~~
- 760 Rubinato, M., Shucksmith, J., Saul, A. J., and Shepherd, W.: Comparison between InfoWorks hydraulic results and a physical model of an urban drainage system, *Water Sci. Technol.*, 68, 372–379, 2013.
- Sakijege, T. and Dakyaga, F.: Going beyond generalisation: perspective on the persistence of urban floods in Dar es Salaam, *Nat. Hazards*, 115, 1909–1926, <https://doi.org/10.1007/s11069-022-05645-9>, 2023.
- 765 Sambe-Ba, B., Espié, E., Faye, M. E., Timbiné, L. G., Sembene, M., and Gassama-Sow, A.: Community-acquired diarrhea among children and adults in urban settings in Senegal: clinical, epidemiological and microbiological aspects, *BMC Infect. Dis.*, 13, 580, <https://doi.org/10.1186/1471-2334-13-580>, 2013.
- Sané, O., Gaye, A. T., Diakhate, M., and Aziadekey, M.: Critical Factors of Vulnerability That Enable Medina Gounass (Dakar/Senegal) to Adapt against Seasonal Flood Events, *J. Geogr. Inf. Syst.*, 08, 457–469, <https://doi.org/10.4236/jgis.2016.84038>, 2016.
- 770 Sane, Y., Panthou, G., Bodian, A., Vischel, T., Lebel, T., Dacosta, H., Quantin, G., Wilcox, C., Ndiaye, O., Diongue-Niang, A., and Diop Kane, M.: Intensity–duration–frequency (IDF) rainfall curves in Senegal, *Nat. Hazards Earth Syst. Sci.*, 18, 1849–1866, <https://doi.org/10.5194/nhess-18-1849-2018>, 2018.
- Sène, A., Sarr, M. A., Kane, A., and Diallo, M.: L’assèchement des lacs littoraux de la grande côte du Sénégal: Mythe ou réalité? Cas des lacs Thiourour, Warouwaye et Wouye de la banlieue de Dakar, *J Anim Plant Sci*, 35, 5623–5638, 2018.
- 775 Sène, A. M.: L’urbanisation de l’Afrique: davantage de bidonvilles ou des villes intelligentes ?, *Popul. Avenir*, 739, 14–16, <https://doi.org/10.3917/popav.739.0014>, 2018.
- Sene, S. and Ozer, P.: Evolution pluviométrique et relation inondations – événements pluvieux au Sénégal, *Bull. Société Géographique Liège*, 42, 2002.
- 780 Sidek, L. M., Jaafar, A. S., Majid, W. H. A. W. A., Basri, H., Marufuzzaman, M., Fared, M. M., and Moon, W. C.: High-resolution hydrological-hydraulic modeling of urban floods using InfoWorks ICM, *Sustainability*, 13, 10259, 2021.

- Šimůnek, J., Genuchten, M. Th., and Šejna, M.: Recent Developments and Applications of the HYDRUS Computer Software Packages, *Vadose Zone J.*, 15, 1–25, <https://doi.org/10.2136/vzj2016.04.0033>, 2016.
- ~~Singh, V. P. and De Lima, J. L. M. P.: One Dimensional Linear Kinematic Wave Solution for Overland Flow under Moving Storms Using the Method of Characteristics, *J. Hydrol. Eng.*, 23, 04018029, [https://doi.org/10.1061/\(ASCE\)HE.1943-5584.0001676](https://doi.org/10.1061/(ASCE)HE.1943-5584.0001676), 2018.~~
- 785 Skrede, T. I., Muthanna, T. M., and Alfredesen, K.: Applicability of urban streets as temporary open floodways, *Hydrol. Res.*, 51, 621–634, <https://doi.org/10.2166/nh.2020.067>, 2020.
- Steenhuis, T. S., Winchell, M., Rossing, J., Zollweg, J. A., and Walter, M. F.: SCS Runoff Equation Revisited for Variable-Source Runoff Areas, *J. Irrig. Drain. Eng.*, 121, 234–238, [https://doi.org/10.1061/\(ASCE\)0733-9437\(1995\)121:3\(234\)](https://doi.org/10.1061/(ASCE)0733-9437(1995)121:3(234)), 1995.
- 790 Sy, B., Frischknecht, C., Dao, H., Consuegra, D., and Giuliani, G.: Reconstituting past flood events: the contribution of citizen science, *Hydrol. Earth Syst. Sci.*, 24, 61–74, <https://doi.org/10.5194/hess-24-61-2020>, 2020.
- ~~Tadesse, A. and Anagnostou, E. N.: African convective system characteristics determined through tracking analysis, *Atmospheric Research*, 98, 468–477, <https://doi.org/10.1016/j.atmosres.2010.08.012>, 2010.~~
- 795 Taromideh, F., Fazloula, R., Choubin, B., Emadi, A., and Berndtsson, R.: Urban Flood-Risk Assessment: Integration of Decision-Making and Machine Learning, *Sustainability*, 14, 4483, <https://doi.org/10.3390/su14084483>, 2022.
- Taylor, C. M., Belušić, D., Guichard, F., Parker, D. J., Vischel, T., Bock, O., Harris, P. P., Janicot, S., Klein, C., and Panthou, G.: Frequency of extreme Sahelian storms tripled since 1982 in satellite observations, *Nature*, 544, 475–478, <https://doi.org/10.1038/nature22069>, 2017.
- 800 Tazen, F., Diarra, A., Kabore, R. F. W., Ibrahim, B., Bologo/Traoré, M., Traoré, K., and Karambiri, H.: Trends in flood events and their relationship to extreme rainfall in an urban area of Sahelian West Africa: The case study of Ouagadougou, Burkina Faso, *J. Flood Risk Manag.*, 12, e12507, <https://doi.org/10.1111/jfr3.12507>, 2018.
- Tramblay, Y., Bouvier, C., Ayral, P.-A., and Marchandise, A.: Impact of rainfall spatial distribution on rainfall-runoff modelling efficiency and initial soil moisture conditions estimation, *Nat. Hazards Earth Syst. Sci.*, 11, 157–170, 805 <https://doi.org/10.5194/nhess-11-157-2011>, 2011.
- ~~Vieux, B. E. and Gauer, N.: Finite Element Modeling of Storm Water Runoff Using GRASS GIS, *Comput. Aided Civ. Infrastruct. Eng.*, 9, 263–270, <https://doi.org/10.1111/j.1467-8667.1994.tb00334.x>, 1994.~~
- Williams, D. S., Mániez Costa, M., Sutherland, C., Celliers, L., and Scheffran, J.: Vulnerability of informal settlements in the context of rapid urbanization and climate change, *Environ. Urban.*, 31, 157–176, 810 <https://doi.org/10.1177/0956247818819694>, 2019.
- Yengoh, G. T., Fogwe, Z. N., and Armah, F. A.: Floods in the Douala metropolis, Cameroon: attribution to changes in rainfall characteristics or planning failures?, *J. Environ. Plan. Manag.*, 60, 204–230, <https://doi.org/10.1080/09640568.2016.1149048>, 2017.

- 815 Yuan, Y., Chen, S. S., and Miao, Y.: Unmanaged Urban Growth in Dar es Salaam: The Spatiotemporal Pattern and Influencing Factors, *Sustainability*, 15, 10575, <https://doi.org/10.3390/su151310575>, 2023.
- Zanchetta, A. and Coulibaly, P.: Recent Advances in Real-Time Pluvial Flash Flood Forecasting, *Water*, 12, 570, <https://doi.org/10.3390/w12020570>, 2020.
- Zhang, C., Huang, H., and Li, Y.: Analysis of water accumulation in urban street based on DEM generated from LiDAR data, *DESALINATION WATER Treat.*, 119, 253–261, <https://doi.org/10.5004/dwt.2018.22049>, 2018.
- 820 Zheng, X., Maidment, D. R., Tarboton, D. G., Liu, Y. Y., and Passalacqua, P.: GeoFlood: Large-Scale Flood Inundation Mapping Based on High-Resolution Terrain Analysis, *Water Resour. Res.*, 54, <https://doi.org/10.1029/2018WR023457>, 2018.
- Zhenyu, X. and Olivier, B.: Conception des réseaux d’assainissement: Pluies de projet et norme NF EN 752-2, *Rev. Eur. Génie Civ.*, 9, 401–413, <https://doi.org/10.1080/17747120.2005.9692762>, 2005.
- 825 Zhu, Z., Chen, Z., Chen, X., and He, P.: Approach for evaluating inundation risks in urban drainage systems, *Sci. Total Environ.*, 553, 1–12, <https://doi.org/10.1016/j.scitotenv.2016.02.025>, 2016.